Experimental Characterization of the Alkene-Addition/-Insertion Energy Profile at Homogeneous Group 4 Metal Ziegler-Type Catalysts

Marc Dahlmann, Gerhard Erker,* and Klaus Bergander

Contribution from the Organisch-Chemisches Institut der Universität Münster, Corrensstrasse 40, D-48149 Münster, Germany

Received February 14, 2000

Abstract: Treatment of the *ansa*-metallocene complex $[Me_2Si(C_5H_4)_2]Zr$(butadiene) (*s-cis*-/*s-trans*-**4**) with $B(C_6F_5)_3$ yields the corresponding *ansa*-zirconocene$[C_4H_6B(C_6F_5)_3]$ betaine **6**. Complex **6** is a homogeneous single component Ziegler catalyst that actively polymerizes ethene and propene, respectively. With the olefins ethene, propene, 1-butene, 1-pentene, 1-hexene, or 1,5-hexadiene complex **6** undergoes a stoichiometric insertion reaction at −20 °C to generate the metallacyclic carbon−carbon coupling products **9a**−**9f**, which feature an internal C4═C5 alkene coordination to the metal center and an intramolecular C6−Zr ion pair interaction. The rate of the overall 1-alkene insertion process **6** → **9** (k_{chem}) was measured, and the observed rate constant of the degenerate allyl inversion process of the starting material (**6** → ent-**6**, $k_{m(obs)}$). This allows for a mathematical kinetic deconvolution of the two-step reaction sequence, namely the initial alkene addition process to **6** to generate the reactive (π-alkene)(σ-allyl)metallocene-type intermediate **8** (rate of formation (k_1[alkene], rate of alkene dissociation: k_{-1}) and the subsequent insertion reaction **8** → **9** (k_2) to give k_1 (= k_{chem} + 2 $k_{m(obs)}$) and the ratio k_2/k_{-1} (= $k_{chem}/2\ k_{m(obs)}$). This procedure quantitatively determines the two transition states involved. In each case of the **6** → **9b**−**f** series the second transition state is higher than the first one: a general energy profile is observed in which the actual insertion step is rate-determining and is preceded by the alkene addition/alkene dissociation preequilibrium. For example, the rate of 1-pentene dissociation at the stage of the intermediate **8** to reform the starting material **6** is ∼70 times higher than the competing actually product forming alkene insertion reaction to yield **9d**. The difference of transition-state energies ranges from $\Delta\Delta G^{\ddagger}_2 = 1.7 \pm 0.4$ kcal mol^{-1} for 1-butene insertion to $\Delta\Delta G^{\ddagger}_2 = 2.1 \pm 0.4$ kcal mol^{-1} for 1-pentene and 1-hexene insertion, respectively. The kinetic analysis of the alkene insertion reaction at the single component "constrained geometry" catalyst $[Me_2Si(C_5H_4)N^tBu]Zr[C_4H_6B(C_6F_5)_3]$ **11** was carried out analogously. $B(C_6F_5)_3$ addition to $[Me_2Si(C_5H_4)N^tBu]Zr$(butadiene) **10** yields a 1.8:1 mixture of the stereoisomeric betaines **11A**/**11B** ("supine/prone" orientation of the ligand). The **11A**/**11B** complex mixture actively polymerizes ethene. At low temperature the **11A**/**11B** mixture reacts stoichiometrically with the series of olefins listed above to give the mono-alkene insertion products **14a**−**f**, each found in solution as a single diastereoisomer. The kinetic analysis shows an even more pronounced alkene addition/alkene dissociation preequilibrium step ($k_{-1}/k_2 \approx$ 130 for 1-pentene) followed by rate-determining insertion ($\Delta\Delta G^{\ddagger}_2$ ranging from +2.2 to +3.0 kcal mol^{-1}). Reaction profiles featuring the actual alkene insertion step as the kinetically controlling activation barrier could be characteristic for group 4 metallocene Ziegler catalysts and related systems.

Introduction

Homogeneous group 4 metal Ziegler-type catalyst systems have gone through some remarkable development recently.[1] They have become generally important catalyst systems that often combine pronounced selectivity features with very high reaction rates. Understanding their action in detail requires an in-depth knowledge about the energy profile of the sequence of alkene addition and subsequent insertion that leads to successive carbon−carbon coupling in the coordination sphere of the active transition metal center. Is it, for instance, the alkene coordination step, followed by rapid insertion to form, for example, the isotactic polypropylene that determines the stereo- and regioselectivity or is there a rapid olefin coordination/dissociation equilibrium preceding an overall rate- and selectivity-determining insertion reaction? Are rotational isomers of different symmetries in an open group 4 metallocene catalyst decisive for elastomeric stereoblock polypropylene formation[2] as it was proposed,[3] or is carbon−carbon coupling insertion so slow relative to metallocene conformational equilibration to create a Curtin-Hammett situation, that would require a different

(1) Sinn, H.; Kaminsky, W. *Adv. Organomet. Chem.* **1980**, *18*, 99−149. Jordan, R. F. *Adv. Organomet. Chem.* **1991**, *32*, 325−387. Marks, T. *J. Acc. Chem. Res.* **1992**, *25*, 57−65. Aulbach, M.; Küber, F. *Chem. Unserer Zeit* **1994**, *28*, 197−208. Brintzinger, H. H.; Fischer, D.; Mülhaupt, R.; Rieger, B.; Waymouth, R. M. *Angew. Chem.* **1995**, *107*, 1255−1283; *Angew. Chem., Int. Ed. Engl.* **1995**, *34*, 1143−1170. Bochmann, M. *J. Chem. Soc., Dalton Trans.* **1996**, 255−270. Kaminsky, W. *J. Chem. Soc., Dalton Trans.* **1998**, 1413−1418. McKnight, A. L.; Waymouth, R. M. *Chem. Rev.* **1998**, *98*, 2587−2598.

(2) Erker, G.; Aulbach, M.; Knickmeier, M.; Wingbermühle, D.; Krüger, C.; Nolte, M.; Werner, S. *J. Am. Chem. Soc.* **1993**, *115*, 4590−4601. Knickmeier, M.; Erker, G.; Fox, T. *J. Am. Chem. Soc.* **1996**, *118*, 9623−9630. See also: Knüppel, S.; Fauré, J.-L.; Erker, G.; Kehr, G.; Nissinen, M.; Fröhlich, R. *Organometallics* **2000**, *19*, 1262−1268. Bruce, M. D.; Coates, G. W.; Hauptmann, E.; Waymouth, R. M.; Ziller, J. W. *J. Am. Chem. Soc.* **1997**, *119*, 11174−11182.

10.1021/ja0005338 CCC: $19.00
Published on Web 08/08/2000

explanation to rationalize the observed phenomenon? The answer to many of these and related questions lies in a quantitative evaluation of the respective energy profiles at the active catalyst systems, which is not a simple task in view of the extremely high reactivity of such homogeneous catalyst systems.[4]

There have been only a few reports in the literature thus far about experimental approaches to determine the activation energies of alkene coordination/dissociation and of alkene insertion into a metal to carbon bond at active homogeneous group 4 metal Ziegler-type catalysts.[5−9] Our system[9] involves the experimental study of the first alkene insertion reaction step in the initial phase of the catalytic sequence at a single component group 4 metal butadiene/$B(C_6F_5)_3$ catalyst system. The system is readily prepared by treatment of, for example, a group 4 metallocene dihalide with butadiene−magnesium[10] to yield the respective (η^4-C_4H_6)$ZrCp_2^R$ complex system.[11] Subsequent $B(C_6F_5)_3$ addition occurs rapidly and selectively leads to the formation of the metallocene−betaine catalyst system **1**.[9,12] The complexes **1** react with a variety of unsaturated substrates, including α-olefins, to form the mono-insertion products **3** selectively at low temperature;[13] increasing the temperature above a specific limit then leads the system into the catalytic cycle of effectively producing the respective polymer.

Scheme 1

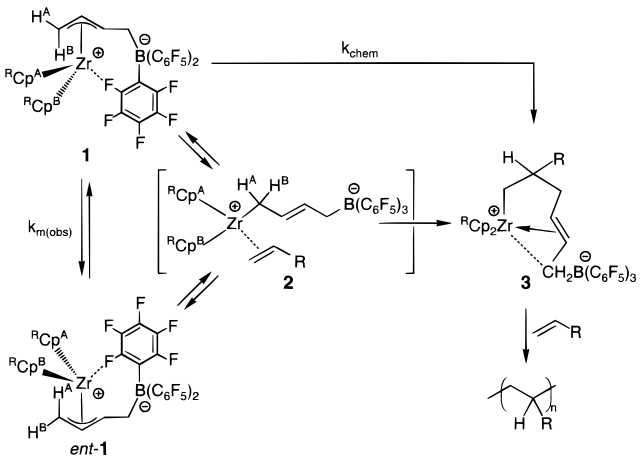

The overall rate constant of the single alkene insertion reaction (k_{chem}, see Scheme 1) was measured for the $(MeCp)_2Zr$ derived system.[9] The reaction is likely to proceed through a reactive (π-alkene)(σ-allyl)metallocene intermediate **2**, that at the same time is the likely intermediate of the thermal, monomer-induced allyl automerization reaction of the starting material **1** which is experimentally followed by dynamic NMR spectroscopy.[14] A special consequence of the kinetically coupled systems (**1** ⇋

(3) Coates, G. W.; Waymouth, R. M. *Science* **1995**, *267*, 217−219. Hauptmann, E.; Waymouth, R. M.; Ziller, J. W. *J. Am. Chem. Soc*. **1995**, *117*, 11586−11587. Maciejewski, J. L.; Bruce, M. D.; Waymouth, R. M.; Masood, A.; Lal, T. K.; Quan, R. W.; Behrend, S. J. *Organometallics* **1997**, *16*, 5909−5916. Tagge, C. D.; Kravchenko, R. L.; Lal, T. K.; Waymouth, R. M. *Organometallics* **1999**, *18*, 380−388.

(4) Theoretical approaches to solving this problem are numerous. For representative examples see: Kawamura-Kuribayashi, H.; Koga, N.; Morokuma, K. *J. Am. Chem. Soc*. **1992**, *114*, 8687−8694. Jensen, V. R.; Ystenes, M.; Wärnmark, K.; Åkermark, B.; Svensson, M.; Siegbahn, P. E. M.; Blomberg, M. R. A. *Organometallics* **1994**, *13*, 282−288. Bierwagen, E. P.; Bercaw, J. E.; Goddard, W. A., III *J. Am. Chem. Soc*. **1994**, *116*, 1481−1489. Yoshida, T.; Koga, N.; Morokuma, K. *Organometallics* **1995**, *14*, 746−758. Fan, L.; Harrison, D.; Woo, T. K.; Ziegler, T. *Organometallics* **1995**, *14*, 2018−2026. Jensen, V. R.; Børve, K. J.; Ystenes, M. *J. Am. Chem. Soc*. **1995**, *117*, 4109−4117. Lohrenz, J. C. W.; Woo, T. K.; Ziegler, T. *J. Am. Chem. Soc*. **1995**, *117*, 12793−12800. Margl, P.; Lohrenz, J. C. W.; Ziegler, T.; Blöchl, P. E. *J. Am. Chem. Soc*. **1996**, *118*, 4434−4441. Richardson, D. E.; Alameddin, N. G.; Ryan, M. F.; Hayes, T.; Eyler, J. R.; Siedle, A. R. *J. Am. Chem. Soc.* **1996**, *118*, 11244−11253. Woo, T. K.; Margl, P. M.; Lohrenz, J. C. W.; Blöchl, P. E.; Ziegler, T. *J. Am. Chem. Soc.* **1996**, *118*, 13021−13030. Guerra, G.; Cavallo, L.; Moscardi, G.; Vacatello, M.; Corradini, P. *Macromolecules* **1996**, *29*, 4834−4845. Froese, R. D. J.; Musaev, D. G.; Matsubara, T.; Morokuma, K. *J. Am. Chem. Soc*. **1997**, *119*, 7190−7196. Margl, P.; Deng, L.; Ziegler, T. *Organometallics* **1998**, *17*, 933−946; *J. Am. Chem. Soc*. **1998**, *120*, 5517−5525. Froese, R. D. J.; Musaev, D. G.; Morokuma, K. *J. Mol. Struct. (THEOCHEM)* **1999**, *461−462*, 121−135.

(5) For other potential model systems, see, e.g.: (a) Horton, A. D. *Organometallics* **1992**, *11*, 3271−3275. Mashima, K.; Fujikawa, S.; Nakamura, A. *J. Am. Chem. Soc.* **1993**, *115*, 10990−10991. Pindado, G. J.; Thornton-Pett, M.; Bowkamp, M.; Meetsma, A.; Hessen, B.; Bochmann, M. *Angew. Chem*. **1997**, *109*, 2457−2460; *Angew. Chem., Int. Ed. Engl*. **1997**, *36*, 2358−2361. (b) Jordan, R. F.; Taylor, D. F. *J. Am. Chem. Soc.* **1989**, *111*, 778−779. Jordan, R. F.; LaPointe, R. E.; Bradley, P. K.; Baenziger, N. *Organometallics* **1989**, *8*, 2892−2903. Jordan, R. F.; Taylor, D. F.; Baenziger, N. C. *Organometallics* **1990**, *9*, 1546−1557. Guram, A. S.; Jordan, R. F.; Taylor, D. F. *J. Am. Chem. Soc*. **1991**, *113*, 1833−1835. Guram, A. S.; Jordan, R. F. *Organometallics* **1991**, *10*, 3470−3479. Pellecchia, C.; Grassi, A.; Zambelli, A. *J. Chem. Soc., Chem. Commun*. **1993**, 947−949. Pellecchia, C.; Grassi, A.; Immirzi, A. *J. Am. Chem. Soc*. **1993**, *115*, 1160−1162. Pellecchia, C.; Immirzi, A.; Grassi, A.; Zambelli, A. *Organometallics* **1993**, *12*, 4473−4478. Alelyunas, Y. W.; Baenziger, N. C.; Bradley, P. K.; Jordan, R. F. *Organometallics* **1994**, *13*, 148−156. Pellecchia, C.; Grassi, A.; Zambelli, A. *Organometallics* **1994**, *13*, 298−302. Guo, Z.; Swenson, D. C.; Jordan, R. F. *Organometallics* **1994**, *13*, 1424−1432. Pellecchia, C.; Immirzi, A.; Pappalardo, D.; Peluso, A. *Organometallics* **1994**, *13*, 3773−3775. Pellecchia, C.; Immirzi, A.; Zambelli, A. *J. Organomet. Chem*. **1994**, *479*, C9−C11. Dagorne, S.; Rodewald, S.; Jordan, R. F. *Organometallics* **1997**, *16*, 5541−5555 and references therein. (c) Fink, G.; Fenzl, W.; Mynott, R. In *Catalytic Polymerization of Olefins*; Kodansha: Tokyo, 1986, p 215−229; Mynott, R.; Fink, G.; Fenzl, W. *Angew. Macromol. Chem.* **1987**, *154*, 1−21.

(6) Wu, Z.; Jordan, R. F.; Petersen, J. L. *J. Am. Chem. Soc.* **1995**, *117*, 5867−5868. Galakhov, M. V.; Heinz, G.; Royo, P. *J. Chem. Soc., Chem. Commun.* **1998**, 17−18.

(7) Casey, C. P.; Hallenbeck, S. L.; Polloch, D. W.; Landis, C. R. *J. Am. Chem. Soc*. **1995**, *117*, 9770−9771. Casey, C. P.; Hallenbeck, S. L.; Wright, J. M.; Landis, C. R. *J. Am. Chem. Soc*. **1997**, *119*, 9680−9690. Casey, C. P.; Fisher, J. *J. Inorg. Chim. Acta* **1998**, *270*, 5−7. Casey, C. P.; Fagan, M. A.; Hallenbeck, S. L. *Organometallics* **1998**, *17*, 287−289. Casey, C. P.; Carpenetti, D. W., II; Sakurai, H. *J. Am. Chem. Soc*. **1999**, *121*, 9483−9484.

(8) (a) Clawson, L.; Soto, J.; Buchwald, S. L.; Steigerwald, M. L.; Grubbs, R. H. *J. Am. Chem. Soc*. **1985**, *107*, 3377−3378. Joung, J. R.; Stille, J. R. *J. Am. Chem. Soc.* **1992**, *114*, 4936−4937. Barta, N. S.; Kirk, B. A.; Stille, J. R. *J. Am. Chem. Soc.* **1994**, *116*, 8912−8919. (b) Piers, W. E.; Bercaw, J. E. *J. Am. Chem. Soc.* **1990**, *112*, 9406−9407. Kraudelat, H.; Brintzinger, H.-H. *Angew. Chem.* **1990**, *102*, 1459−1460; *Angew. Chem., Int. Ed. Engl*. **1990**, *29*, 1417−1418. Leclerc, M. K.; Brintzinger, H.-H. *J. Am. Chem. Soc.* **1995**, *117*, 1651−1652; *J. Am. Chem. Soc.* **1996**, *118*, 9024−9032. (c) Feichtinger, D.; Plattner, D. A.; Chen, P. *J. Am. Chem. Soc*. **1998**, *120*, 7125−7126.

(9) Karl, J.; Dahlmann, M.; Erker, G.; Bergander, K. *J. Am. Chem. Soc.* **1998**, *120*, 5643−5652.

(10) Ramsden, H. E. U.S. Patent 3,388,179, 1968. Nakano, Y.; Natsukawa, K.; Yasuda, H.; Tani, H. *Tetrahedron Lett.* **1972**, 2833−2836. Fujita, K.; Ohnuma, Y.; Yasuda, H.; Tani, H. *J. Organomet. Chem.* **1976**, *113*, 201−213. Yasuda, H.; Nakano, Y.; Natsukawa, K.; Tani, H. *Macromolecules* **1978**, *11*, 586−592. Kai, Y.; Kanehisa, N.; Miki, K.; Kasai, N.; Mashima, K.; Yasuda, H.; Nakamura, A. *Chem. Lett*. **1982**, 1277−1280.

(11) Erker, G.; Krüger, C.; Müller, G. *Adv. Organomet. Chem*. **1985**, *24*, 1−39 and references therein. Erker, G.; Wicher, J.; Engel, K.; Rosenfeldt, F.; Dietrich, W.; Krüger, C. *J. Am. Chem. Soc*. **1980**, *102*, 6344−6346. Erker, G.; Wicher, J.; Engel, K.; Krüger, C. *Chem. Ber.* **1982**, *115*, 3300−3310. Erker, G.; Engel, K.; Krüger, C.; Chiang, A.-P. *Chem. Ber*. **1982**, *115*, 3311−3323. Yasuda, H.; Kajihara, Y.; Mashima, K.; Nagasuna, K.; Lee, K.; Nakamura, A. *Organometallics* **1982**, *1*, 388−396. Bürgi, T.; Berke, H.; Wingbermühle, D.; Psiorz, C.; Noe, R.; Fox, T.; Knickmeier, M.; Berlekamp, M.; Fröhlich, R.; Erker, G. *J. Organomet. Chem*. **1995**, *497*, 149−159.

(12) Temme, B.; Erker, G.; Karl, J.; Luftmann, H.; Fröhlich, R.: Kotila, S. *Angew. Chem*. **1995**, *107*, 1867−1869; *Angew. Chem., Int. Ed. Engl*. **1995**, *34*, 1755−1757. Karl, J.; Erker, G.; Fröhlich, R. *J. Am. Chem. Soc*. **1997**, *119*, 11165−11173.

(13) Temme, B.; Karl, J.; Erker, G. *Chem. Eur. J*. **1996**, *2*, 919−924. Karl, J.; Erker, G. *Chem. Ber./Recl.* **1997**, *130*, 1261−1267. Karl, J.; Erker, G. *J. Mol. Catal*. **1998**, *128*, 85−102.

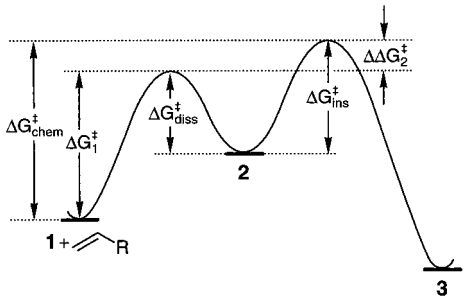

Figure 1. Energy profile determined at the $(MeCp)_2Zr[C_4H_6B(C_6F_5)_3]$ betaine single component metallocene Ziegler catalyst system **1**.

ent-**1**) ⇌ **2** → **3** is that the observed rate of the dynamic NMR experiment ($k_{m(obs)}$, measured by magnetization transfer within pairs of diastereotopic groups in the course of the **1** ⇌ ent-**1** interconversion) is dependent on the actual rate k_{chem} of the irreversible chemical reaction of **1** leading to **3** at the specific reaction temperature. Using the experimentally determined rate constants k_{chem} and $k_{m(obs)}$ it was possible to deconvolute the energy profile of a single alkene addition/insertion step at the $(MeCp)_2Zr[C_4H_6B(C_6F_5)_3]$ single component Ziegler catalyst for a variety of α-olefin insertions and determine $\Delta G^{\ddagger}_1$ and $\Delta\Delta G_2^{\ddagger}$ with a reasonable accuracy (see Figure 1, see the Supporting Information for a detailed error estimation and calculation of all catalyst systems described and discussed in this article). In each case it turned out that the alkene coordination step is taking place as a preequilibrium step, followed by rate-determining alkene insertion. Alkene dissociation from the intermediate at this specific system is kinetically favored by a factor of 3 over insertion for propene [k_{diss}:k_{ins} = 8 (butene), 5 (pentene)].

This posed the question whether a rapid alkene coordination/dissociation preequilibrium is typical for the possible manifold of such homogeneous group 4 metal single component Ziegler-type catalyst systems or if the $(MeCp)_2Zr$-derived nonbridged metallocene system represented a special exceptional case. The most often used catalyst systems are derived from *ansa*-metallocenes[1,15] or silylene-bridged Cp/amido metal complex systems.[16,17] We, therefore, applied the derived method for the energy profile analysis of a typical single component "constrained geometry" catalyst and a silylene-bridged *ansa*-metallocene catalyst system. The outcome of this study points to some generality of the results obtained at the $(MeCp)_2Zr$-derived catalyst, although some interesting differences were observed among this series of catalyst systems.

Scheme 2

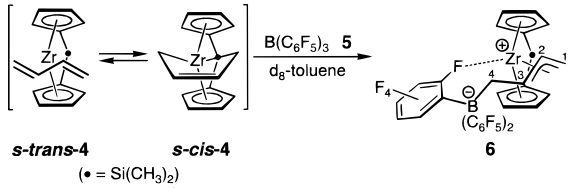

Results and Discussion

Alkene Insertion into the *ansa*-Metallocene Betaine System 6. Reaction of the *s-cis*- and *s-trans*-$[Me_2Si(C_5H_4)_2]Zr$(butadiene) complex mixture[19,20] (**4**) with $B(C_6F_5)_3$ (**5**)[18] in toluene solution led to the clean formation of the 1:1 addition product **6** (Scheme 2) that contains a distorted *E*-π-allyl unit[21] and one short (aryl)C−F···metal interaction[12,20] (characterized by X-ray diffraction and an NMR analysis).

The planar-chiral Zr−(C1,C2,C3) allyl moiety of betaine **6** undergoes a dynamic configurational inversion in solution by which complex **6** is interconverted with its enantiomer, ***ent*-6**. This automerization reaction probably proceeds via a (σ-allyl)-zirconocene intermediate (**7**, see Scheme 3).[22] The electron-deficient zirconium center in **7** might be stabilized by solvatization. The dynamic process leads to a marked broadening of the ^{1}H NMR signals of the allyl-CH_2-borate ligand at temperatures above 300 K (200 MHz). However, we were not able to determine the activation energy by conventional dynamic ^{1}H NMR spectroscopy due to the inset of a fast competing irreversible chemical rearrangement reaction at the allyl moiety below the coalescence temperature (in d_8-toluene).

As described previously by us for the $(MeCp)_2Zr[C_4H_6B(C_6F_5)_3]$ betaine system, the dynamic process can be monitored quantitatively at lower temperatures by using a one-dimensional NMR spin saturation transfer experiment.[23] By this method the transition of a specific proton between two diastereotopic positions in the **6**/***ent*-6** system is followed by means of the transfer of magnetization between these two sites. In the case of the **6** ⇌ ***ent*-6** reaction the diastereotopic allyl-1-H_{syn}/1-H_{anti} protons were suited for this experiment. Thus, magnetic

(14) (a) Hoffmann, E. G.; Kallweit, R.; Schroth, G.; Seevogel, K.; Stempfle, W.; Wilke, G. *J. Organomet. Chem.* **1975**, *97*, 183−202. (b) Erker, G.; Berg, K.; Krüger, C.; Müller, G.; Angermund, K.; Benn, R.; Schroth, G. *Angew. Chem.* **1984**, *96*, 445−446; *Angew. Chem., Int. Ed. Engl.* **1984**, *23*, 455−456. Erker, G.; Berg, K.; Angermund, K.; Krüger, C. *Organometallics* **1987**, *6*, 2620−2621. (c) Abrams, M. B.; Yoder, J. C.; Loeber, C.; Day, M. W.; Bercaw, J. E. *Organometallics* **1999**, *18*, 1389−1401 and references therein.

(15) Bajgur, C. S.; Tikkanen, W. R.; Petersen, J. L. *Inorg. Chem.* **1985**, *24*, 2539−2546.

(16) (a) Shapiro, P. J.; Cotter, W. D.; Schaefer, W. P.; Labinger, J. A.; Bercaw, J. E. *J. Am. Chem. Soc.* **1994**, *116*, 4623−4640. Piers, W. E.; Shapiro, P. J.; Bunel, E. E.; Bercaw, J. E. *Synlett* **1990**, *2*, 74−84. Bunel, E. E.; Burger, B. J.; Bercaw, J. E. *J. Am. Chem. Soc.* **1988**, *110*, 976−978. Shapiro, P. J.; Bunel, E. E.; Schaefer, W. P.; Bercaw, J. E. *Organometallics* **1990**, *9*, 867−869. (b) Stevens, J. C.; Timmers, F. J.; Wilson, D. R.; Schmidt, G. F.; Nickias, P. N.; Rosen, R. K.; Knight, G. W.; Lai, S. (Dow Chemical Co.). Eur. Pat. Appl. EP 416815-A2, 1991; Canich, J. M. (Exxon Chemical Co.). Eur. Pat. Appl. EP 420436-A1, 1991; Canich, J. M.; Hlatky, G. G.; Turner, H. W. PCT Appl. WO 92-00333, 1992.

(17) Duda, L.; Erker, G.; Fröhlich, R.; Zippel, F. *Eur. J. Inorg. Chem.* **1998**, 1153−1162. Bertuleit, A.; Könemann, M.; Duda, L.; Erker, G.; Fröhlich, R. *Top. Catal.* **1999**, *7*, 37−44.

(18) (a) Massey, A. G.; Park, A. J.; Stone, F. G. A. *Proc. Chem. Soc.* London **1963**, 212. Massey, A. G.; Park, A. J. *J. Organomet. Chem.* **1964**, *2*, 245−250. Massey, A. G.; Park, A. J. In *Organometallic Syntheses*; King, R. B., Eisch, J. J., Eds.; Elsevier: New York, 1986, Vol. 3, pp 461−462. (b) Warning: the in situ generated LiC_6F_5 reagent is potentially explosive and should be handled with due care! (c) See also: Kehr, G.; Fröhlich, R.; Erker, G. *Chem. Eur. J.* **2000**, *6*, 258−266.

(19) Böhme, U.; Thiele, K.-H.; Rufinska, A. *Z. Anorg. Allg. Chem.* **1994**, *620*, 1455−1462.

(20) Dahlmann, M.; Erker, G.; Fröhlich, R.; Meyer, O. *Organometallics* **2000**. In press.

(21) Brauer, D. J.; Krüger, C. *Organometallics* **1982**, *1*, 207−210. Erker, G.; Engel, K.; Dorf, U.; Atwood, J. L.; Hunter, W. E. *Angew. Chem.* **1982**, *94*, 915−916; *Angew. Chem., Int. Ed. Engl.* **1982**, *21*, 914−915. Larson, E. J.; Van Dort, P. C.; Dailey, J. S.; Lakanen, J. R.; Pederson, L. M.; Silver, M. E.; Huffman, J. C.; Russo, S. O. *Organometallics* **1987**, *6*, 2141−2146. Larson, E. J.; Van Dort, P. C.; Lakanen, J. R.; O'Neill, D. W.; Pederson, L. M.; McCandless, J. J.; Silver, M. E.; Russo, S. O.; Huffman, J. C. *Organometallics* **1988**, *7*, 1183−1187. Erker, G. *Angew. Chem.* **1989**, *101*, 411−426; *Angew. Chem., Int. Ed. Engl.* **1989**, *28*, 397−412. Hauger, B. E.; Vance, P. J.; Prins, T. J.; Wemple, M. E. M.; Kort, D. A.; Silver, M. E.; Huffman, J. C. *Inorg. Chim. Acta*, **1991**, *187*, 91−97.

(22) A reviewer expressed concern that the **6** ⇌ ent-**6** interconversion might proceed through a chelate η^1-allyl-zirconium intermediate that still contained the Zr−F−C interaction. This seems unlikely in view of the markedly *lower* activation barrier of Zr−F fission (**6**: $\Delta G^{\ddagger}_{F-Zr\ diss}$ (250 K) = 8.7 ± 0.4 kcal/mol[20]) relative to the automerization barrier of **6** ($\Delta G^{\ddagger}_{m(solv)}$ (243 K) = 14.6 ± 0.3 kcal/mol).

(23) Forsén, S.; Hoffman, R. A. *J. Chem. Phys.* **1963**, *39*, 2892−2901. Baine, P.; Gerig, J. R.; Stock, A. D. *Org. Magn. Reson.* **1981**, *17*, 41−45. Martin, M. L.; Delpuech, J.-J.; Martin, G. J. In *Practial NMR Spectroscopy*; Heyden: London, 1980; pp 315−321.

Scheme 3

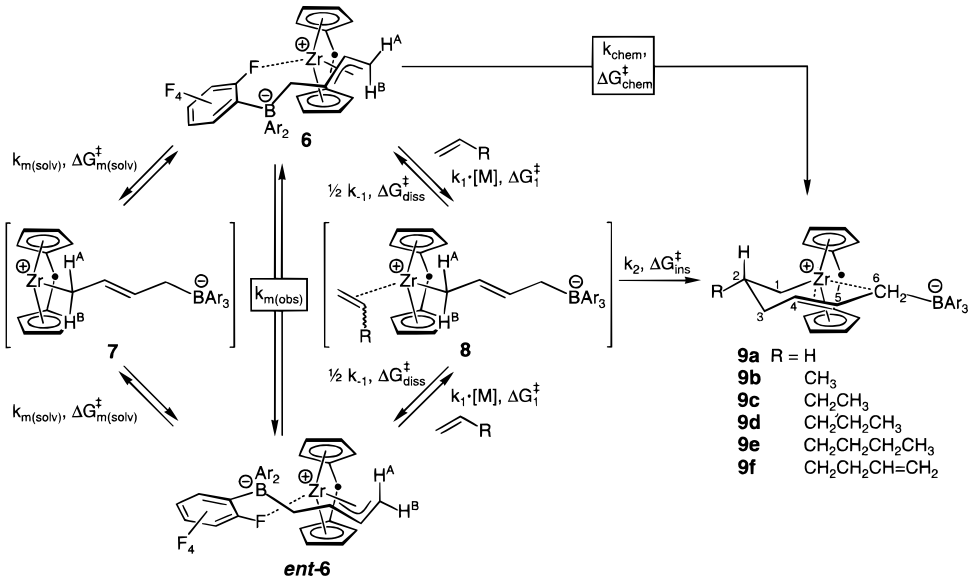

saturation of 1-H_{anti} by irradiation at its ^{1}H NMR resonance frequency leads to a relative decrease in the intensity of the 1-H_{syn} signal because the allyl automerization process equilibrates the specific 1-H_{anti} and 1-H_{syn} positions. If we name M_{0A} the magnetization of the observed 1-H_{syn} signal *without* prior irradiation of the 1-H_{anti} resonance frequency, $M_{zA\infty}$ the magnetization of 1-H_{syn} *with* prior irradiation (irradiation time $t \rightarrow \infty$) and T_{1A} the longitudinal relaxation time of 1-H_{syn}, then the following quantitative description for the lifetime τ_A of **6** and thus the rate constant k_A of the **6** → ***ent*-6** interconversion can be deduced.[9,23]

$$\frac{1}{\tau_A} = k_A = \frac{M_{0A} - M_{zA\infty}}{M_{zA\infty} \cdot T_{1A}} \qquad (1)$$

By means of this method a rate constant of $k_{m(solv)}(T) = 0.35$ s^{-1} was determined for the **6** → ***ent*-6** automerization process at $T = 243$ K in toluene-d_8 solution. The corresponding Gibbs activation energy for this first-order reaction amounts to $\Delta G^{\ddagger}_{m(solv)}$ (243 K) = 14.6 ± 0.3 kcal/mol.

Betaine complex **6** is an active single component Ziegler catalyst for the polymerization of ethene and propene. At a reaction temperature of 40 °C ethene is rapidly polymerized in toluene solution with an activity of >1500 g of polyethylene/mmol [Zr]·bar·h (mp 125 °C). Polymerization of propene under analogous reaction conditions gives polypropylene with an activity of 38 g of polypropylene/mmol [Zr]·bar·h. Because of the lack of stereochemical information in the [$Me_2Si(C_5H_4)_2$]-Zr *ansa*-metallocene backbone the resulting polymer is atactic (2.5% isotactic [*mmmm*] ^{13}C NMR methyl pentade intensity[24]).

The [$Me_2Si(C_5H_4)_2$]Zr[$C_4H_6B(C_6F_5)_3$] Ziegler catalyst system **6** can also be reacted with 1-alkenes stoichiometrically in a 1:1 ratio and the mono-olefin insertion product kept stable and observed experimentally at low temperature. This was achieved by the addition of a slight excess of the respective alkene to a solution of **6** in toluene-d_8 at −30 to −40 °C. In this study, ethene and the α-olefins propene, 1-butene, 1-pentene, and 1-hexene as well as 1,5-hexadiene were used. The NMR spectroscopic analysis of the reaction mixtures revealed the clean formation of the metallacyclic mono-olefin insertion products **9a**−**f**, which are thermally labile but could be adequately characterized at low temperature using a combination of one- and two-dimensional NMR spectroscopic techniques. In this series (see Scheme 3) the insertion reaction proceeds with very high regio- and stereoselectivity. Clean [1,2]-insertion of these α-olefins into the Zr−C bond of **6** is observed, which makes the alkyl group R end up in the *β*-position to the transition metal center in the products **9b**−**f**, that is, at carbon atom C2. Stereocontrol in these cases is equally pronounced to probably result in a favored pseudoequatorial orientation of the substituent R at the crown-shaped metallacyclic [Zr]−CH_2CHRCH_2CH═$CHCH_2$−[B] ring system of the resulting products. The ^{1}H and ^{13}C NMR spectroscopic signal pattern of the C1−C6 alkyl chain is very similar in the series of products **9a**−**f**, indicating a common structure of these compounds, characterized by coordination of the C(4)═C(5) double bond to zirconium, and an internal C(6)−Zr ion pair interaction as it is typical for this class of compounds[6,7,13,25,26] (for details see the Experimental Section).

Complex **9f** was obtained by the stoichiometric reaction of the betaine complex **6** with 1,5-hexadiene in a 1:1 ratio. It exhibits NMR spectra similar to those of the products **9a**−**e** of stoichiometric mono-olefin insertions. The ^{13}C NMR spectra of **9b** gave no indication of any interaction of the remaining terminal −CH═CH_2 group with the metal center.

Kinetic Evaluation of the Alkene Insertion Reactions. The reaction of betaine **6** with the α-olefins was kinetically monitored in the following way: complex **6** was generated in situ in a toluene-d_8 solution that contained an accurately measured concentration of ferrocene as an internal standard (concentration of **6** ~8 *μ*mol/ml). An aliquot of this solution was transferred to an NMR tube and cooled to −60 °C. An excess of the alkene was added to ensure pseudo-first-order kinetic conditions for the alkene insertion reaction. The NMR tube was then sealed and brought to the reaction temperature (243 K) inside the probe of an NMR spectrometer. The decrease of the concentration of **6** was followed by recording one scan (^{1}H) per minute and integration of its Si(CH_3)$_2$ signals against

(24) ^{13}C NMR methyl pentade analysis: Bovey, F. A.; Tiers, G. C. D. *J. Polym. Sci.* **1960**, *44*, 173−182. Sheldon, R. A.; Fueno, T.; Tsuntsuga, R.; Kurukawa, J. *J. Polym. Sci., Part B* **1965**, *3*, 23−26. Zambelli, A.; Locatelli, P.; Bajo, G.; Bovey, F. A. *Macromolecules* **1975**, *8*, 687−689. Farina, M. *Top. Stereochem.* **1987**, *17*, 1−111. For the statistical treatment see: Inoue, J.; Itabashi, Y.; Chujo, R.; Doi, Y. *Polymer* **1984**, *25*, 1640−1644. Erker, G.; Nolte, R.; Tsay, Y.-H.; Krüger, C. *Angew. Chem.* **1989**, *101*, 642−644; *Angew. Chem., Int. Ed. Engl.* **1989**, *28*, 628−629.

Table 1. Characterization of Essential Rate Constants and Gibbs Activation Energies in the Betaine-Catalyst/1-Alkene Reaction Systems

catalyst	alkene	T_{chem}(K)[a]	k_{chem} [b]	$\Delta G^{\ddagger}_{chem}$ [c]	T_m(K)[d]	$k_{m(obs)}$ [e]	k_{chem} [e]	k_1 [e]	Δ	$\Delta G^{\ddagger}_1$ [c]	$\Delta\Delta G^{\ddagger}_2$ [c]
6	propene	243	$2.99\cdot10^{-1}$	14.7							
	1-butene	243	$2.21\cdot10^{-1}$	14.9	243	3.46	$2.21\cdot10^{-1}$	7.15	$3.19\cdot10^{-2}$	13.2(4)[f]	1.7(4)
	1-pentene	243	$8.22\cdot10^{-2}$	15.3	243	2.87	$8.22\cdot10^{-2}$	5.82	$1.43\cdot10^{-2}$	13.3(3)	2.1(3)
	1-hexene	243	$5.43\cdot10^{-2}$	15.5	243	1.91	$5.43\cdot10^{-2}$	3.88	$1.42\cdot10^{-2}$	13.5(4)	2.1(4)
11A/11B	ethene	253	$4.80\cdot10^{-3}$	17.4							
	propene	273	$5.22\cdot10^{-3}$	18.8	278	0.40	$9.92\cdot10^{-3}$	0.80	$1.25\cdot10^{-2}$	16.4(1)	2.4(1)
	1-butene	273	$3.80\cdot10^{-3}$	19.0	288	0.97	$2.47\cdot10^{-2}$	1.97	$1.27\cdot10^{-2}$	16.5(5)	2.5(5)
	1-pentene	288	$5.74\cdot10^{-3}$	19.8	288	0.37	$5.74\cdot10^{-3}$	0.74	$7.81\cdot10^{-3}$	17.0(2)	2.8(2)
	1-hexene	293	$3.31\cdot10^{-3}$	20.5	288	0.17	$1.77\cdot10^{-3}$	0.34	$5.29\cdot10^{-3}$	17.5(6)	3.0(7)
	1,5-hexadiene[g]	273	$1.43\cdot10^{-3}$	19.5	288	0.22	$9.78\cdot10^{-3}$	0.45	$2.20\cdot10^{-2}$	17.3(2)	2.2(2)

[a] Temperature at which k_{chem} was determined. [b] At T_{chem}, in L/mol·s. [c] ±0.1 kcal/mol, calcd for standard state conditions of $c^{\ominus} = 1$ mol/L. [d] Temperature at which $k_{m(obs)}$ was determined. [e] At T_m, in L/mol·s, see the Supporting Information for error calculation. [f] That is 13.2 ± 0.4 kcal/mol. [g] Each value calcd for one of the two double bonds.

Table 2. Comparison of Characteristic Gibbs Activation Energies in the Betaine-Catalyst/1-Alkene Reaction Systems[a]

catalyst	inserted monomer	$\Delta G^{\ddagger}_{chem}$ [b]	$\Delta G^{\ddagger}_1$	$\Delta\Delta G^{\ddagger}_2$	$\Delta G^{\ddagger}_{m(solv)} - \Delta G^{\ddagger}_1$	$\Delta G^{\ddagger}_{diss}$	$\Delta G^{\ddagger}_{ins}$	k_{-1}/k_2 [c]
$(MeCp)_2Zr(C_4H_6)/B(C_6F_5)_3$ (**1**)[d]	propene	17.3	16.5(5)	0.7(5)	3.3(5)	10.2(7)	10.9(9)	3
	1-butene	18.4	17.1(5)	1.2(5)	2.7(5)	9.6(7)	10.8(9)	8
	1-pentene	18.8	17.7(5)	1.0(5)	2.1(5)	9.0(7)	10.0(9)	5
$[Me_2SiCp_2]Zr(C_4H_6)/B(C_6F_5)_3$ (**6**)	1-butene	14.9	13.2(4)	1.7(4)	1.5(4)	9.0(6)	10.6(8)	31
	1-pentene	15.3	13.3(3)	2.1(3)	1.4(3)	8.9(6)	10.9(7)	70
	1-hexene	15.5	13.5(4)	2.1(4)	1.2(4)	8.7(7)	10.7(8)	70
$[Me_2Si(C_5Me_4)(N^tBu)]Zr(C_4H_6)/B(C_6F_5)_3$ (**11A/11B**)	propene	18.8	16.4(1)	2.4(1)	1.2(1)	7.3(5)	9.8(5)	80
	1-butene	19.0	16.5(5)	2.5(5)	1.2(5)	7.3(7)	9.8(9)	79
	1-pentene	19.8	17.0(2)	2.8(2)	0.6(2)	6.7(6)	9.5(6)	128
	1-hexene	20.5	17.5(6)	3.0(7)	0.1(6)	6.2(8)	9.2(10)	189
	1,5-hexadiene	19.5	17.3(2)	2.2(2)	0.3(2)	6.4(5)	8.6(6)	45

[a] $\Delta G^{\ddagger}$-values in kcal/mol, calculated for standard state conditions of $c^{\ominus} = 1$ mol/L, temperatures as given in Table 1. [b] ±0.1 kcal/mol. [c] See the Supporting Information for a detailed error calculation. [d] For details see ref 9.

the ferrocene signal. Under the conditions chosen for these experiments, the reaction was complete within ~20 min. Each kinetic experiment was repeated to check the reproducibility of the obtained results. The reaction of **6** with ethene and 1,5-hexadiene proved to be too fast to be reproduced with the necessary accuracy (see Tables 1 and 2 and the Supporting Information for calculated errors).

From the experimental data the pseudo-first-order rate constants $k_{c(exp)}$ were calculated. Division by the respective monomer concentration, [**M**], gave the second-order rate constants $k_{chem}(T)$ of the overall chemical reaction **6** + **M** → **9** and the corresponding Gibbs activation energies $\Delta G^{\ddagger}_{chem}(T)$ (see Table 1). For propene, a rather low activation barrier of $\Delta G^{\ddagger}_{chem}$ (243 K) = 14.7 ± 0.1 kcal/mol was determined. On going to the higher homologues, a small increase of this value can be observed (1-butene: $\Delta G^{\ddagger}_{chem}$(243 K) = 14.9, 1-pentene: 15.3, 1-hexene: 15.5 (± 0.1) kcal/mol). The decreasing reactivity of the betaine **6** toward α-olefins with increasing length of their alkyl substituent chain corresponds to the behavior of typical metallocene Ziegler catalyst systems, although the *ansa*-metallocene ligand framework of **6** seems to be less sensitive in this respect compared to, for example, the $(MeCp)_2Zr$-(butadiene)/$B(C_6F_5)_3$ catalyst system **1** (see Table 2).[9]

The activation energy $\Delta G^{\ddagger}_{chem}$ corresponds to the energy difference between the highest point on the potential surface along the reaction pathway taken in the overall insertion reaction **6** + **M** → **9** and the energy of the starting materials, **6** + **M** (see Scheme 1). However, one cannot conclude *a priori* which of the two consecutive reaction steps, namely the formation of the alkene complex **8** from **6** plus alkene or the subsequent CC-coupling step starting from the intermediate **8** and leading to **9**, is the actual rate determining step of the overall reaction sequence. This question can be answered by using the unique features of the homogeneous (butadiene)metallocene/$B(C_6F_5)_3$/alkene Ziegler systems.[9] It is very likely that the alkene complex **8**, which is the essential reactive intermediate in the alkene insertion reaction leading to **9**, is also involved in the allyl automerization process of betaine **6** in the presence of an 1-alkene. This provides us principally with an opportunity to determine the activation energy $\Delta G^{\ddagger}_1$ of the formation of **8** (see Scheme 3) by monitoring the rate of the reversible **6** ⇌ ***ent*-6** interconversion by an NMR spin saturation transfer experiment in the presence of the reactive 1-alkene. However, the experimental situation becomes complicated by the competing irreversible chemical insertion reaction **6** + **M** → **9** that leads to a rapid decrease of the concentration of **6** and therefore only allows for a limited number of measurements. The spin saturation transfer experiments were thus repeated twice to ensure reproducibility of the obtained rate constants. However, the chemical reaction of **6** with propene leading to **9b** proved to be too fast for a reliable application of this technique.

We must note two additional more severe complications: (1) the pseudo-first-order rate constants determined by eq 1, which we name $k_{m(exp)}$ in this specific case, cannot be used directly to calculate $\Delta G^{\ddagger}_1$. If we compare the rate of the dynamic **6** ⇌ ***ent*-6** interconversion in the absence of a reactive 1-alkene (i.e, $k_{m(solv)}$) and in the presence of an added alkene (i.e., $k_{m(exp)}$) we note that a significant increase in the automerization rate is observed in the latter case, but both values are still within the same order of magnitude (for details see the Experimental Section). This means that the automerization of the allyl ligand in **6** can take place by two competing mechanisms, namely via a (σ-allyl)(π-alkene)metallocene complex **8** and alternatively an (σ-allyl)metallocene complex **7**, that is only stabilized by solvatization (see Scheme 3). To obtain the rate constant of the first process, i.e., the **6** + **M** → **8** → ***ent*-6** + **M** conversion, the value of $k_{m(exp)}$ has to be reduced by the rate of the nonalkene accelerated process, $k_{m(solv)}$. Division by the monomer concen-

tration [**M**] gives the second-order rate constant $k_{m(obs)}$ for the automerization via an alkene complex:

$$k_{m(obs)} = \frac{k_{m(exp)} - k_{m(solv)}}{[M]} \quad (2)$$

(2) A second necessary correction of $k_{m(obs)}$ arises from the fact that in the presence of a reactive alkene the configurational inversion of the allyl ligand (**6** → ***ent*-6**) and the chemical insertion reaction (**6** + **M** → **9**) are no longer independent processes. The alkene insertion reaction into the Zr−C σ-bond of **8** leads to a decrease in the concentration of **8** and thus an apparent lowering of the $k_{m(obs)}$ value. We, therefore, have to take the kinetic dependency of these two processes into account by connecting the rate expressions of the automerization process **6** + **M** → **8** → ***ent*-6** + **M**

$$\frac{d[\textbf{ent-6}]}{dt} = k_{m(obs)}[\textbf{6}][\textbf{M}] = k_1[\textbf{6}][\textbf{M}] - k_2[\textbf{8}] - \frac{1}{2}k_{-1}[\textbf{8}] \quad (3)$$

and the chemical insertion reaction **6** + **M** → **8** → **9**

$$-\frac{d[\textbf{6}]}{dt} = k_{chem}[\textbf{6}][\textbf{M}] = k_1[\textbf{6}][\textbf{M}] - k_{-1}[\textbf{8}] \quad (4)$$

with the steady-state condition for the reactive intermediate **8**

$$\frac{d[\textbf{8}]}{dt} = k_1[\textbf{6}][\textbf{M}] - k_{-1}[\textbf{8}] - k_2[\textbf{8}] = 0 \quad (5)$$

This leads to a simple expression for the actual rate constant k_1 of the formation of the alkene complex **8**

$$k_1 = k_{chem} + 2k_{m(obs)} \quad (6)$$

and the ratio Δ of the rates of olefin insertion from **8** to give the carbon−carbon coupling product **9** and alkene dissociation, that leads back to the starting materials.[27]

$$\Delta = \frac{k_2}{k_{-1}} = \frac{k_{chem}}{2k_{m(obs)}} \quad (7)$$

The values for $k_{m(obs)}$, k_1, and Δ obtained by this method as well as the respective energy values $\Delta G^{\ddagger}_1$ (calculated from k_1, see Scheme 3) and $\Delta\Delta G^{\ddagger}_2$ (calculated from $\Delta = k_2/k_{-1}$) are listed in Table 1.

A significant acceleration of the dynamic **6** → ***ent*-6** allyl automerization process is observed in the presence on an added 1-alkene compared to the situation in pure toluene. For example, in the presence of 0.015 mol/L 1-butene, the pseudo-first-order rate constant $k_{m(exp)} = 0.42\ s^{-1}$ is ∼18% higher than the corresponding value in the pure arene solvent ($k_{m(solv)} = 0.35\ s^{-1}$, for standard deviations see the Supporting Information). We must assume that this rate acceleration is due to a mechanistic pathway that proceeds through a (π-alkene)(σ-allyl)-metallocene intermediate (**8**). In **8**, the σ-allyl complex is stabilized by the coordinated alkene relative to the alkene-free intermediate **7**, which is at the most stabilized by solvatization. Thus, the activation energy of the formation of **8** should be markedly lower than that of the formation of **7**. This aspect is quantitatively reflected by the values of $\Delta G^{\ddagger}_1$ calculated from the experimental data. Compared to the activation energy of the formation of **7** ($\Delta G^{\ddagger}_{m(solv)} = 14.6 \pm 0.3$ kcal/mol), the formation of **8** requires the lower activation energy $\Delta G^{\ddagger}_1$. The amount of this decrease in the energy barrier depends on the size of the alkene. It is most pronounced in the case of 1-butene ($\Delta G^{\ddagger}_{m(solv)} - \Delta G^{\ddagger}_1 = 1.5 \pm 0.4$ kcal/mol) and slightly decreases on going to the higher homologues 1-pentene (1.4 ± 0.3 kcal/mol) and 1-hexene (1.2 ± 0.4 kcal/mol).[28] However, the dependency of these values on the monomer size is much less pronounced than in the $(MeCp)_2Zr[(\mu\text{-}C_4H_6)B(C_6F_5)_3]$ betaine catalyst system **1** previously described by us.[9]

We must note that for each alkene examined a positive value of $\Delta\Delta G^{\ddagger}_2$ was found. This means that the transition state of the insertion of the alkene into the Zr−C bond at the stage of the (π-alkene)(σ-allyl)metallocene complex **8** represents the highest point on the energy surface of the overall reaction sequence and, therefore, makes overcoming the alkene insertion barrier the rate determining step. In other words, dissociation of the alkene complex **8**, once formed from betaine complex **6** and the alkene, into the starting materials proceeds more rapidly than the alkene insertion to yield the metallacyclic products **9**. The ratio of the two corresponding reaction rates, $1/\Delta = k_{-1}/k_2$, ranges from ∼30 (1-butene) to ∼70 (1-pentene and 1-hexene) (see Table 2).

Characterization of the Alkene Insertion Energy Profile at a Constrained Geometry Single Component Ziegler Catalyst System. The silylene-bridged Cp-amido group 4 metallocenes are the basis of an important class of homogeneous Ziegler-type catalysts ("constrained geometry catalysts").[16,17] The mixture of isomeric [dimethylsilylene(tetramethylcyclopentadienyl)(*tert*-butylamido)](*s-cis*-butadiene)zirconium complexes **10A/10B**[29] also reacts cleanly with $B(C_6F_5)_3$ in aromatic solvents to yield two diastereomeric addition products **11A** and **11B** in a ratio of ∼65:35 (see Scheme 4).[30] However, the structure of these betainic complexes differs in some details from that of the betainic *ansa*-metallocene **6** and its congeners. Both compounds **11A/11B** exhibit overall C_1 symmetry, indicated by a set of each four ^1H and ^{13}C NMR resonances of the cyclopentadienyl methyl groups and pairs of resonances for the methyl groups of the silylene bridge for each complex. In both cases the borane has added to the CH_2 terminus of the butadiene ligand. The ^{13}C NMR resonances of the methylene group α- to boron appear at δ ∼25 (**11A**) and ∼31 (**11B**) ppm. The remaining three carbon atoms of the C_4-units form π-allyl systems coordinated to zirconium. In contrast to betaine **6**, the allyl ligand in both **11A** and **11B** is *anti* substituted, that is, it exhibits a *Z*-configuration at the central C2,C3 π-bond.[31−33] This

(25) (a) Dahlmann, M.; Erker, G.; Nissinen, M.; Fröhlich, R. *J. Am. Chem. Soc*. **1999**, *121*, 2820−2828. (b) See also: Gilchrist, J. H.; Bercaw, J. E. *J. Am. Chem. Soc.* **1996**, *118*, 12021−12028. Sacchi, M. C.; Barsties, E.; Tritto, I.; Locatelli, P.; Brintzinger, H.-H.; Stehling, U. *Macromolecules* **1997**, *30*, 3955−3957. (c) Sacchi, M. C.; Locatelli, P.; Tritto, I. *Makromol. Chem*. **1989**, *190*, 139−143.

(26) Yang, X.; Stern, C. L.; Marks, T. J. *J. Am. Chem. Soc.* **1994**, *116*, 10015−10031. Schottek, J.; Erker, G.; Fröhlich, R. *Angew. Chem*. **1997**, *109*, 2585−2587; *Angew. Chem., Int. Ed. Engl*. **1997**, *36*, 2475−2477. Beswick, C. L.; Marks, T. J. *Organometallics* **1999**, *18*, 2410−2412.

(27) The derivation of $k_{m(obs)}$ given in our initial paper[9] should be corrected by the statistical factor of 1/2. The resulting marginally different $\Delta G^{\ddagger}$ values of the $(MeCp)_2Zr[C_4H_6B(C_6F_5)_3]$ betaine + alkene reactions are listed in Table 2.

(28) These $\Delta G^{\ddagger}_{m(solv)} - \Delta G^{\ddagger}_1$ values probably represented a good measure of the alkylmetallocene cation/π-alkene stabilization energies in these systems. For a discussion see also refs 6 and 7.

(29) Dahlmann, M.; Schottek, J.; Fröhlich, R.; Kunz, D.; Nissinen, M.; Erker, G.; Fink, G.; Kleinschmidt, R. *J. Chem. Soc., Dalton Trans*. **2000**, 1881−1886.

(30) Devore, D. D.; Timmers, F. J.; Hasha, D. L.; Rosen, R. K.; Marks, T. J.; Deck, P. A.; Stern, C. L. *Organometallics* **1995**, *14*, 3132−3134.

(31) See for a comparison: Karl, J.; Erker, G.; Fröhlich, R.; Zippel, F.; Bickelhaupt, F.; Schreuder Goedheijt, M.; Akkerman, O. S.; Binger, P.; Stannek, *Angew. Chem*. **1997**, *109*, 2914−2917; *Angew. Chem., Int. Ed. Engl*. **1997**, *36*, 2771−2774.

(32) Karl, J.; Erker, G.; Fröhlich, R. *J. Organomet. Chem*. **1997**, *535*, 59−62.

Scheme 4

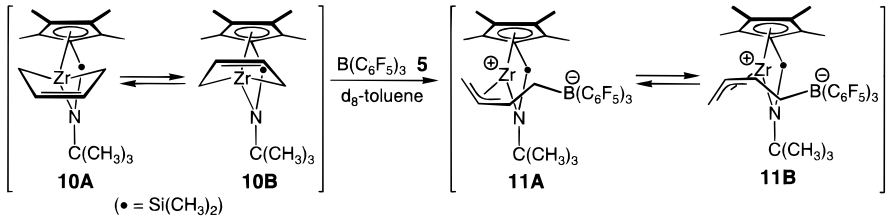

Scheme 5

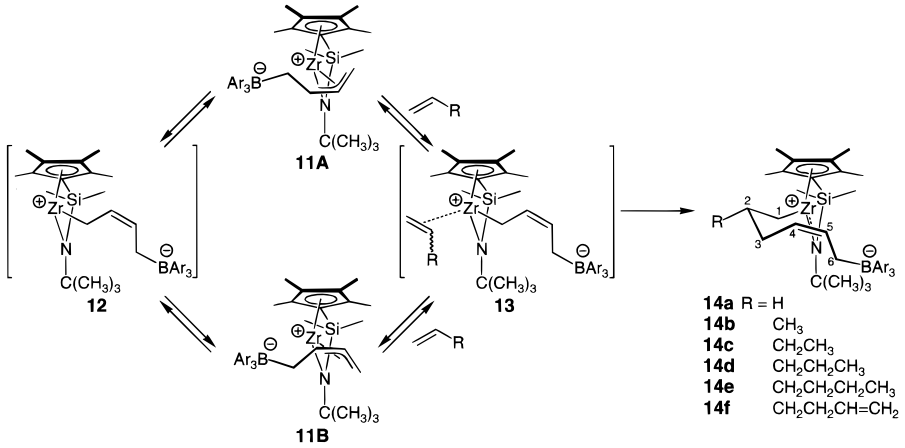

becomes evident from the ^{1}H NMR signals of the corresponding protons 2-H and 3-H (δ 6.54 and 5.13 (**11A**); δ 5.23 and 4.02 (**11B**)), which show a $^3J_{2-H,3-H}$ coupling constant of 9.3 (**11A**) and 9.8 (**11B**) Hz, respectively.[20] The two diastereomers thus only differ in the configuration of the planar chiral C1,C2,C3,-Zr allyl unit relative to the configuration of the stereogenic zirconium center: in one of these complexes the central allylic proton 2-H points toward the cyclopentadienyl ligand ("prone"-orientation), while it is oriented toward the amido group in the other diastereomer ("supine").[34] NOE NMR experiments indicate that the former situation is given in the minor isomer **11B**, while the latter geometry is adopted by the major isomer **11A**. Internal C−F coordination to zirconium is absent in **11A**/**11B** as a geometric consequence of the *Z*-allyl unit as shown by ^{19}F NMR spectroscopy.

The mutual interconversion of the isomeric betaines **11A** and **11B**, which involves an inversion of the planar chiral allyl unit, is too slow to be observed directly by dynamic NMR spectroscopy at variable temperatures. However, this process was monitored using the ^{1}H NMR spin saturation transfer experiment. The two well separated −C(C*H*$_3$)$_3$ ^{1}H NMR resonances of the isomers **11A** and **11B** were used for this purpose. A first-order rate constant $k_{m(solv)}$ (303 K) = 1.28 s^{-1} was determined in toluene-d_8 solution, giving a Gibbs activation energy of $\Delta G^{\ddagger}_{m(solv)}$(303 K) = 17.6 ± 0.2 kcal/mol for this specific catalyst system.

The [Me$_2$Si(C$_5$Me$_4$)(N^{t}Bu)]Zr-derived betaines **11A/11B** show a much lower activity in the Ziegler polymerization of ethene compared to the *ansa*-metallocene **6**. At a reaction temperature of 40 °C, only traces of polyethylene could be isolated. At 90 °C, ethene is polymerized in toluene solution with an activity of ∼390 g of polyethylene/mmol [Zr]·bar·h.

The stoichiometric reaction of **11A/11B** with alkenes proceeds much slower than that of the *ansa*-metallocene **6**. Only ethene and 1,5-hexadiene react spontaneously with **11A/11B** to form the respective mono-insertion products, **14a** and **14f**, respectively (see Scheme 5). The reactions with propene, 1-butene, 1-pentene, or 1-hexene require a prolonged reaction time of ∼8 h at −20 °C to go to completion. The employed α-olefins react regioselectively ([1,2]-insertion) and stereoselectively within the limits of detection. In each case only a single diastereomerically pure reaction product is formed that contains only one combination of relative configurations of the three stereogenic units present in the products, namely the chiral zirconium center, the planar chiral substituted allyl moiety and, in the case of **14b**−**f**, the stereogenic center at C2. The metallacyclic insertion products **14a**−**f** exhibit similar spectroscopic properties within this homologous series. In contrast to the complexes **9a**−**f** described above, the C(4)═C(5) double bonds in the corresponding mono-insertion products **14a**−**f** are *Z* configurated. This becomes evident from the characteristic values of the $^3J_{4-H,5-H}$ coupling constants ranging from 12.0 (**14a**) to 10.5 (**14f**) Hz.

The products **14** are chiral (C_1 symmetry). Consequently, they exhibit ^{1}H/^{13}C NMR signals of diastereotopic methyl groups at their cyclopentadienyl ligands and at their silylene bridges. The chemical shifts of the olefinic carbon atoms C4 and C5 of these products again indicate internal coordination of the C═C bond to the transition metal center.[6]

Rate constants k_{chem} and the corresponding activation energies $\Delta G^{\ddagger}_{chem}$ for the 1-alkene insertion into the Zr−C bond of **11A**/**11B**, leading to the products **14**, were determined analogously as described for the *ansa*-metallocene complex **6** (see Table 1). A constant ratio of **11A** and **11B** was maintained during the course of the reaction, indicating identical reactivities of both diastereomers. These kinetic studies (Table 1) have revealed a lower reactivity of the **11A/11B** catalysts compared to the *ansa*-metallocene system **6**. For the reaction of **11A**/**11B** with ethene a second-order rate constant k_{chem} = 4.80·10^{-3} L/mol·s was determined at 253 K, corresponding to a Gibbs activation energy of $\Delta G^{\ddagger}_{chem}$ (253 K) = 17.4 ± 0.1 kcal/mol. The insertion reactions of propene and 1-butene proceed significantly slower.

(33) Cowley, A. H.; Hair, G. S.; McBurnett, B. G.; Jones, R. A. *J. Chem. Soc., Chem. Commun.* **1999**, 437.

(34) For the "prone" and "supine" definition see: Yasuda, H.; Tatsumi, K.; Okamoto, T.; Mashima, K.; Lee, K.; Nakamura, A.; Kai, Y.; Kanehisa, N.; Kasai, N. *J. Am. Chem. Soc.* **1985**, *107*, 2410−2422.

Activation energies of $\Delta G^{\ddagger}_{chem}$ (273 K) = 18.8 and 19.0 (± 0.1) kcal/mol, respectively, were obtained for these monomers. An even higher energy barrier must be overcome for the insertion of the higher homologues 1-pentene ($\Delta G^{\ddagger}_{chem}$ (288 K) = 19.8 ± 0.1 kcal/mol) and 1-hexene ($\Delta G^{\ddagger}_{chem}$ (293 K) = 20.5 ± 0.1 kcal/mol). In the case of 1,5-hexadiene, a value of $2.86 \cdot 10^{-3}$ L/mol·s was obtained for k_{chem} at 273 K. With a statistical factor of 0.5, to account for the presence of two reactive C=C double bonds in the diene, a Gibbs activation energy of $\Delta G^{\ddagger}_{chem}$ (273 K) = 19.5 ± 0.1 kcal/mol was obtained in this case.

The rate of the dynamic **11A** ⇌ **11B** interconversion was again studied in the presence of the reactive alkenes using the NMR spin saturation transfer experiment. Ethene insertion leading to **14a** was proceeding too rapidly to allow for a sufficient lifetime of the betaines **11A/11B** in the presence of this reactive alkene to carry out this NMR experiment. In the presence of propene, an averaged rate constant $k_{m(obs)}$ = 0.40 L/mol·s was determined at 278 K using eq 1. The presence of the higher homologues 1-butene, 1-pentene, 1-hexene, and 1,5-hexadiene results in a smaller acceleration of the **11A** ⇌ **11B** isomerization. At 288 K, $k_{m(obs)}$ values of 0.97, 0.37, 0.17, and 0.22 L/mol·s were obtained, respectively, the latter value again was calculated taking into account that two reactive double bonds are present in this diene.

Although the interconverting metallocene[$C_4H_6B(C_6F_5)_3$] betaine isomers **11A** and **11B** are diastereomers and not energetically identical enantiomers, as in the case of betaine **6**, eqs 6 and 7 can still be used for the kinetic analysis of the **11A/11B** plus 1-alkene reactions.[35] The values obtained for k_1 are listed in Table 1. Again, a significant acceleration of the **11A** ⇌ **11B** allyl isomerization rate is found in the presence of the 1-alkenes, which can be attributed to an energetically favorable mechanistic isomerization pathway that involves the alkene metal complexes **13** as intermediates. The activation energies $\Delta G^{\ddagger}_1$ of the formation of **13** are markedly lower (16.4−17.5 (±0.1 − ±0.6) kcal/mol) than of the formation of the alkene-free intermediate **12** ($\Delta G^{\ddagger}_{m(solv)}$ (303 K) = 17.6 ± 0.2 kcal/mol). Moreover, a distinctive dependence on the size of the 1-alkene is displayed in the experimental values. In this series, the lowest energy barrier $\Delta G^{\ddagger}_1$ was determined for propene ($\Delta G^{\ddagger}_1$ (278 K) = 16.4 ± 0.1 kcal/mol). Increasing the size of the substituent at the 1-alkene results in an increase of this value ($\Delta G^{\ddagger}_1$: 1-butene: 16.5 ± 0.5, 1-pentene: 17.0 ± 0.2, 1-hexene: 17.5 ± 0.6 kcal/mol at 288 K). Increasing steric interaction between the monomer and ligand system at this catalyst may account for this behavior. Especially in the latter cases, this leads to a situation in which the activation energy of the formation of alkene complex **13** is only marginally energetically preferred over the formation of the "unstabilized" intermediate **12** ($\Delta G^{\ddagger}_{m(solv)} - \Delta G^{\ddagger}_1$ = 1.2 (propene), 1.2 (1-butene), 0.6 (1-pentene), 0.1 (1-hexene) kcal/mol, for calculated errors see Table 2).

Similarly as in the case of the *ansa*-metallocene betaine catalyst **6**, in the 1-alkene/Cp-amido-halfsandwich complex **11A/11B** system the transition state of alkene insertion lies higher than the alkene coordination/dissociation transition state. The differences between these two saddle points are $\Delta\Delta G^{\ddagger}_2 = \Delta G^{\ddagger}_{chem} - \Delta G^{\ddagger}_1$ = 2.4 ± 0.1 (propene), 2.5 ± 0.5 (1-butene), 2.8 ± 0.2 (1-pentene), and 3.0 ± 0.7 (1-hexene) kcal/mol. Thus, alkene dissociation from the intermediate **13** is markedly preferred over alkene insertion ($1/\Delta = k_{-1}/k_2$ = ~80 (propene and 1-butene), ~130 (1-pentene), and ~190 (1-hexene)) in this constrained geometry Ziegler catalyst system.

Scheme 6

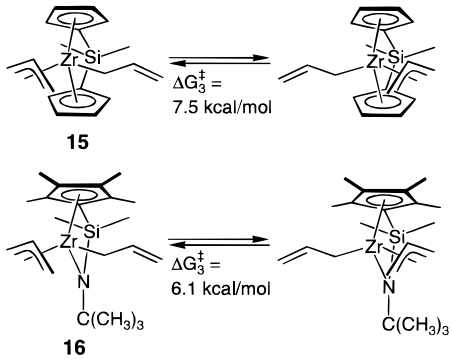

A Rough Estimate of the Alkene Insertion Barrier $\Delta G^{\ddagger}_{ins}$. Since we cannot directly determine the energetic position of the (π-alkene)(σ-allyl)metal complex intermediates **8** and **13** experimentally, we will try to estimate this value using a simple consideration.[9] Going back from, for example, **8** to **6** + **M** requires dissociation of the coordinated alkene and an isomerization of the allyl-CH_2-borate ligand from a σ- to a π-allyl bonding mode. If we assume in a first approximation that about one-half of the π-alkene-zirconium stabilization is lost at the transition state of the **8** → **6** + **M** dissociation, then the energy difference $\Delta G^{\ddagger}_{m(solv)} - \Delta G^{\ddagger}_1$ serves as a rough estimate for the remaining noncompensated fraction of the stabilization energy of the electron-deficient cationic zirconium center in **8** by the coordinated alkene.[6,7,36]

The energetic contribution of the change in the allyl ligand bonding mode was to a first approximation estimated by using the bis(allyl)zirconium complexes **15** and **16** as model compounds (see Scheme 6). These complexes contain a η^3-π-allyl ligand and a η^1-σ-allyl ligand bonded to zirconium.[37] In solution, a rapid intramolecular degenerated isomerization process takes place which is characterized by a mutual interconversion of the σ- and π-allyl ligands. We were able to "freeze out" this dynamic process on the ^{1}H NMR time scale using a $CDCl_2F$/$CDClF_2$ solvent mixture.[38] In the case of *ansa*-metallocene **15**, below a coalescence temperature of ~162 K two diastereotopic methyl groups at the silylene bridge as well as two sets of signals for the allyl ligands can be observed in the ^{1}H NMR spectrum. A Gibbs activation energy of $\Delta G^{\ddagger}_3$ (162 K) = 7.5 ± 0.5 kcal/mol was determined. The automerization of the pair of allyl ligands in the halfsandwich complex **16** is even faster. Coalescence of the $Si(CH_3)_2$ signals is reached at ~130 K, which leads to an activation energy of $\Delta G^{\ddagger}_3$ (130 K) ≈ 6.1 ± 0.5 kcal/mol.

(35) To simplify the mathematical treatment of the (**11A/11B**)/1-alkene reaction system it was assumed that **11A** and **11B** exhibit the same energy content and reactivity. Both assumptions should be justified by the experimental observation of an equilibrium constant [**11A**]/[**11B**] close to unity, which does not change upon the addition of a reactive 1-alkene.

(36) The intrinsic stabilization energy of a [$Cp_2ZrR(\pi$-alkene)$^+$] cation complex is very low because of the lacking metal-to-ligand back-donation in the d°-system. See for a comparison: Hurlburt, P. K.; Rack, J. J.; Luck, J. S.; Dec, S. F.; Webb, J. D.; Anderson, O. P.; Strauss, S. H. *J. Am. Chem. Soc*. **1994**, *116*, 10003−10014. Aubke, F.; Wang, C. *Coord. Chem. Rev.* **1994**, *137*, 483−524. Antonelli, D. M.; Thaden, E. B.; Stryker, J. M. *Organometallics* **1994**, *13*, 763−765. Goldman, A. S.; Krogh-Jespersen, K. *J. Am. Chem. Soc.* **1996**, *118*, 12159−12166. Willner, H.; Aubke, F. *Angew. Chem.* **1997**, *109*, 2507−2530; *Angew. Chem., Int. Ed. Engl*. **1997**, *36*, 2402−2425. Brackemeyer, T.; Erker, G.; Fröhlich, R. *Organometallics* **1997**, *16*, 531−536. Szilagyi, R. K.; Frenking, G. *Organometallics* **1997**, *16*, 4807−4815. Brackemeyer, T.; Erker, G.; Fröhlich, R.; Prigge, J.; Peuchert, U. *Chem. Ber./Recl.* **1997**, *130*, 899−902. Jacobsen, H.; Berke, H.; Brackemeyer, T.; Eisenblätter, T.; Erker, G.; Fröhlich, R.; Meyer, O.; Bergander, K. *Helv. Chim. Acta* **1998**, *81*, 1692−1709.

(37) Tjaden, E. B.; Stryker, J. M. *J. Am. Chem. Soc.* **1993**, *115*, 2083−2085. Tjaden, E. B.; Casty, G. L.; Stryker, J. M. *J. Am. Chem. Soc*. **1993**, *115*, 9814−9815.

(38) Siegel, J. S.; Anet, F. A. L. *J. Org. Chem*. **1988**, *53*, 2629−2630.

Using these experimental values, we estimated the activation energy of alkene dissociation from the (π-alkene)(σ-allyl)metal complex intermediates **8** and **13**, respectively,

$$\Delta G^{\ddagger}_{\mathrm{diss}} \approx \Delta G^{\ddagger}_{3} + (\Delta G^{\ddagger}_{\mathrm{m(solv)}} - \Delta G^{\ddagger}_{1}) \qquad (8)$$

and, consequently, the activation energy of olefin insertion:

$$\Delta G^{\ddagger}_{\mathrm{ins}} \approx \Delta G^{\ddagger}_{\mathrm{diss}} + \Delta\Delta G^{\ddagger}_{2} \qquad (9)$$

Values in the range between ~9−11 kcal/mol were thus estimated for the intrinsic alkene insertion barriers ($\Delta G^{\ddagger}_{\mathrm{ins}}$) at these catalyst systems.[4,7] A complete listing of the characteristic energy values describing the alkene addition/insertion profile of the betaine catalysts **6** and **11A/11B** is given in Table 2 and compared with those of the unbridged parent system **1**.[9]

Conclusions

Obtaining direct experimental evidence about the essential alkene complexation/insertion sequence at a homogeneous Ziegler catalyst is very difficult because the alkene carbon−carbon coupling reactions at such catalyst systems are extremely fast processes.[4,5] Our metallocene[$C_4H_6B(C_6F_5)_3$] betaine systems are probably among the best suited active catalysts at present, where it is possible to kinetically isolate a single alkene insertion reaction sequence in the initial phase leading to the repetitive catalytic cycle, and study this essential step experimentally. The first alkene insertion at the metallocene[$C_4H_6B(C_6F_5)_3$] betaine systems is kinetically separated by internal coordination effects from the subsequent multiple alkene insertions; the subsequent alkene insertion intermediates have not experimentally been observed so far in these systems.[39]

The metallocene[$C_4H_6B(C_6F_5)_3$] betaine/alkene reaction is also unique as it allows for a kinetic deconvolution of the alkene addition/alkene insertion reaction profile and thus a mathematical separation of the characteristic kinetic and energetic features of the two individual steps of the sequence. The specific features of the metallocene[$C_4H_6B(C_6F_5)_3$] betaine plus alkene systems would principally allow, to the best of our knowledge for the first time, to determine the difference between the height of the first transition state (here the alkene addition) and the second transition state (here the actual alkene insertion) even if the latter would be energetically *lower* than the former. In our initial report about a first example of these unique systems[9] we have, however, found that at the $(MeC_5H_4)_2Zr[C_4H_6B(C_6F_5)_3]$ betaine catalyst system the actual alkene insertion step is overall rate determining. At this nonbridged metallocene catalyst system the transition state of the preceding alkene coordination is by ~1 kcal/mol lower in energy (see Table 2).

Our current study, described in this article, now has revealed that this situation seems to be quite general for homogeneous Ziegler catalyst systems containing the most relevant ligand backbones, namely the *ansa*-metallocenes and the Cp-amido systems. Both representative examples described in this study show Curtin-Hammett behavior,[40] being characterized by a rapid alkene complexation/dissociation equilibrium that precedes the rate determining carbon−carbon coupling process. For the *ansa*-metallocene system, the alkene decomplexation reaction is 30−70 times more frequent than productive alkene insertion; in the constrained geometry catalyst system this ratio can approach a value of $k_{-1}/k_2 \approx 200$. This situation is *a priori* valid for our specific examples of the metallocene betaine Ziegler catalysts (**1**, **6**, **11**) in their stoichiometric initiation step. However, it may well be that these experimentally characterized systems are close to be representative for the general alkene addition/insertion steps at these and related homogeneous Ziegler catalysts. The respective (σ-alkyl)(π-alkene)M intermediates (**2**, **8**, **13**) are energetically well separated from both their stable educts and products, and, thus the respective transition states ($TS^{\ddagger}_{\mathrm{diss}}$, $TS^{\ddagger}_{\mathrm{ins}}$) are early transition states, which are consequently not profiting much from the coordinative extra-stabilization features of neither the betaine educts (**1**, **6**, **11**) nor their mono-insertion products (**3**, **9**, **14**). In addition, both the betaine educts and their respective mono-alkene insertion products exhibit energetic stabilization effects which are not much different from each other.

If such a kinetically relevant preequilibrium situation indeed prevails for the majority of relevant types of homogeneous metallocene Ziegler catalysts and related systems, then their characteristic features (stereoselectivity, regiochemistry, chemoselectivity etc.)[1,41] seems to be dominantly governed by the essential interactions between catalyst backbone, growing polymer chain and the *coordinated* alkene in the actual alkene *insertion* step, and not in the alkene coordination process, as it is often assumed. Mechanistic descriptions of a variety of details at the metallocene and related Ziegler catalyst systems should, therefore, take this potentially rather general overall appearance of the alkene addition/alkene insertion profile into account.

Experimental Section

General remarks. All manipulations involving air-sensitive compounds were carried out under argon in a glovebox or using Schlenk type glassware. Solvents (including deuterated solvents) were dried and distilled under argon prior to use. Tris(pentafluorophenyl)borane,[18] [dimethylsilylenebis(cyclopentadienyl)]dichlorozirconium,[15] and [dimethylsilylene(tetramethylcyclopentadienyl)(*tert*-butylamido)]dichlorozirconium[16] were prepared according to literature procedures. The synthesis of [dimethylsilylenebis(cyclopentadienyl)](butadiene)zirconium **4**[19,20,41,42] and [dimethylsilylene(tetramethylcyclopentadienyl)(*tert*-butylamido)](butadiene)zirconium **10B/10B**[29] was described previously by us. NMR experiments were performed on Varian Unity Plus 600 spectrometer (^{1}H: 600 MHz, ^{13}C: 150 MHz, ^{19}F: 564 MHz). Assignments in ^{1}H and ^{13}C NMR spectra were confirmed through GCOSY (gradient ^{1}H−^{1}H COSY), 1D-TOCSY (^{1}H total correlation spectroscopy), GHSQC (^{1}H−^{13}C gradient heteronuclear single quantum coherence), and GHMBC (^{1}H−^{13}C gradient heteronuclear multiple bond correlation) spectra.[43] IR spectra were aquired on a Nicolet 5 DXC Fourier transform IR spectrometer. Melting points were obtained by differential scanning calorimetry (DuPont 910), elemental analyses were determined on a Foss-Heraeus CHN-Rapid elemental analyzer.

Reaction of $[Me_2Si(C_5H_4)_2]$Zr(butadiene) 4 with $B(C_6F_5)_3$. Formation of 6. For this study, betaine complex **6** was generated in situ by adding a solution of $B(C_6F_5)_3$ (31 mg, 60.5 μmol) in 0.4 mL of toluene-d_8 (or C_6D_6) to a solution of butadiene complex **4** (20 mg, 60.3 μmol) in 0.8 mL of toluene-d_8 (or C_6D_6) at room temperature. After mixing, the resulting orange-red solution was allowed to stand at room temperature for ~30 min prior to the spectroscopic characterization of **2** and its reaction with alkenes. The generation and characterization of betaine **6** on a preparative scale was described previously by us.[20] ^{1}H NMR (599.9 MHz, C_6D_6, 298 K): δ = 6.11, 6.00 (each m, each 1H,

(39) Double alkyne insertion products have been isolated in a few related cases, see e.g.: Horton, A. D.; Orpen, A. G. *Organometallics* **1992**, *11*, 8−10.

(40) Curtin, D. Y. *Rec. Chem. Prog.* **1954**, *15*, 111. Seemann J. I. *Chem. Rev.* **1983**, *83*, 83.

(41) Busico, V.; Cipullo, R. *J. Am. Chem. Soc.* **1994**, *116*, 9329−9330. Resoni, L.; Fait, A.; Piemontesi, F.; Colonnesi, M.; Rychlicki, H.; Zeigler, R. *Macromolecules* **1995**, *28*, 6667−6676. Veghini, D.; Henling, L. M.; Burkhardt, T. J.; Bercaw, J. E. *J. Am. Chem. Soc.* **1999**, *121*, 564−573.

(42) Dahlmann, M.; Erker, G.; Fröhlich, R.; Meyer, O. *Organometallics* **1999**, *18*, 4459−4461.

(43) Braun, S.; Kalinowski, H.-O.; Berger, S. *150 and More Basic NMR Experiments*; VCH: Weinheim, 1998 and references therein.

C_5H_4), 5.92 (m, 2H, C_5H_4 and 2-H), 5.78 (1H), 5.55 (2H) (each m, C_5H_4), 5.43 (m, 1H, 3-H), 4.40 (m, 2H, C_5H_4), 2.63 (broad d, ^2J = 18.2 Hz, 1H, 4-H), 2.31 (broad dd, ^2J = 18.2 Hz, ^3J = 6.0 Hz, 1H, 4-H′), 1.86 (dd, ^2J = 5.0 Hz, ^3J = 17.9 Hz, 1H, 1-H), 1.53 (dd, ^2J = 5.0 Hz, ^3J = 8.3 Hz, 1H, 1-H′), 0.24, −0.17 (each s, each 3H, Si-$(CH_3)_2$). ^{13}C NMR (150.8 MHz, C_6D_6, 298 K): δ = 149.5 (d, $^1J_{CF}$ = 240 Hz, *o*-B$(C_6F_5)_3$), 138.9 (d, $^1J_{CF}$ = 250 Hz, *p*-B$(C_6F_5)_3$), 137.3 (d, $^1J_{CF}$ = 250 Hz, *m*-B$(C_6F_5)_3$), 130.4 (CH_2, broad, C-2), 125.8 (C, broad, ipso-B$(C_6F_5)_3$), 125.1, 123.7 (each CH, α- or *β*-C_5H_4), 123.1 (CH, broad, C-3), 121.9, 121.2, 109.9, 107.2 (double intensity), 106.6 (each CH, α- or *β*-C_5H_4), 106.1, 102.7 (each C, ipso-C_5H_4), 52.0 (CH_2, C-1), 28.3 (CH_2, broad, C-4), −5.7, −7.1 (each CH_3, Si$(CH_3)_2$). ^{19}F NMR (564.3 MHz, toluene-d_8, 298 K): δ = −165.0 (broad, 6F, *m*-F), −161.1 (broad t, $^3J_{FF}$ = 21 Hz, 3F, *p*-F) ppm, *o*-F signals not detected at 298 K. ^{19}F NMR (564.3 MHz, toluene-d_8, 238 K): δ = −211.6 (broad, 1F, *o*-F (coordinated)), −165.4, −163 to −157 (each broad m, 9F, *m*-F and *p*-F), −125.8 (1F), −132.7 (4F) (each broad, *o*-F). Coalescence of the *o*-F signals is reached at ∼250 K, $\Delta\nu$ (238 K) ∼45500 Hz, $\Delta G^{\ddagger}$ (250 K) = (8.7 ± 0.4) kcal/mol.

Reaction of [Me$_2$Si(C$_5$Me$_4$)(N^{t}Bu)]Zr(butadiene) 10A/10B with B(C$_6$F$_5$)$_3$: Formation of 11A/11B. For this study, betaine **11** was generated in situ by the addition of a solution of butadiene zirconium complex **10** (22 mg, 55.7 μmol) in 3 mL of C_6D_6 or toluene-d_8 to a solution of B$(C_6F_5)_3$ (29 mg, 56.6 μmol) in 2 mL of C_6D_6 or toluene-d_8. An aliquot of this solution was used for the reaction of **11** with 1-alkenes and for the kinetic measurements. The formation of two diastereomeric betaines **11A** and **11B** in a ratio of 1.8:1 can be observed by NMR spectroscopy. **11A:** ^{1}H NMR (599.9 MHz, C_6D_6, 298 K): δ = 6.54 (m, $^3J_{2,1}$ = 9.5 Hz, $^3J_{2,1'}$ = 13.2 Hz, $^3J_{2,3}$ = 9.3 Hz, 1H, 2-H), 5.13 (m, $^3J_{3,2}$ = 9.3 Hz, $^4J_{3,1}$ = 2.1 Hz, $^4J_{3,1'}$ = 2.4 Hz, 1H, 3-H), 2.17 (m, $^2J_{1,1'}$ = 6.4 Hz, $^3J_{1,2}$ = 9.5 Hz, $^4J_{1,3}$ = 2.1 Hz, 1H, 1-H), 2.07, 1.82, 1.59, 1.39 (each s, each 3H, $C_5(CH_3)_4$), 1.19 (m, $^2J_{1',1}$ = 6.4 Hz, $^3J_{1',2}$ = 13.2 Hz, $^4J_{1',3}$ = 2.4 Hz, $^5J_{1',4}$ = 1.8 Hz, 1H, 1-H′), 1.00 (broad m, 1H, 4-H), 0.80 (s, 9H, C$(CH_3)_3$), 0.43, 0.19 (each s, each 3H, Si$(CH_3)_2$), −0.18 (broad m, 1H, 4-H′). ^{13}C NMR (150.8 MHz, C_6D_6, 298 K): δ = 149.5 (d, $^1J_{CF}$ = 240 Hz, *o*-B$(C_6F_5)_3$), 139.4 (d, $^1J_{CF}$ = 250 Hz, *p*-B$(C_6F_5)_3$), 137.5 (d, $^1J_{CF}$ = 250 Hz, *m*-B$(C_6F_5)_3$), 145.5 (CH, C-2), 131.8, 130.9 (each C, α- and *β*-$\underline{C}_5(CH_3)_4$), 116.9 (CH, C-3), 109.9 (C, ipso-$\underline{C}_5(CH_3)_4$), 68.1 (CH_2, C-1), 60.6 (C, $\underline{C}(CH_3)_3$), 34.6 (CH_3, C$(\underline{C}H_3)_3$), ∼25 (CH_2, C-4), 14.8, 13.2, 11.1, 10.2 (each CH_3, α- and *β*-$\underline{C}_5(\underline{C}H_3)_4$), 8.2, 5.4 (each CH_3, Si$(CH_3)_2$), resonance of the ipso-C of B$(C_6F_5)_3$ not detected, resonance of C-4 only detected in the GHSQC spectrum. ^{19}F NMR (564.3 MHz, toluene-d_8, 273 K): δ = −164.8 (broad, 6F, *m*-F), −160.1 (broad t, $^3J_{FF}$ = 20 Hz, 3F, *p*-F), −137.8 (broad, 6F, *o*-F).

11B: ^{1}H NMR (599.9 MHz, C_6D_6, 298 K): δ = 5.23 (m, $^3J_{2,1}$ = 9.8 Hz, $^3J_{2,1'}$ = 12.8 Hz, $^3J_{2,3}$ = 9.8 Hz, 1H, 2-H), 4.02 (m, $^3J_{3,2}$ = 9.8 Hz, $^3J_{3,4}$ = 13.3 Hz, 1H, 3-H), 2.26 (m, $^2J_{1,1'}$ = 7.3 Hz, $^3J_{1,2}$ = 9.8 Hz, 1H, 1-H), 2.04 (m, $^2J_{1',1}$ = 7.3 Hz, $^3J_{1',2}$ = 12.8 Hz, 1H, 1-H′), 1.90, 1.48 (each s, each 3H, $C_5(CH_3)_4$), 1.38 (under signal of isomer **11A**, 1H, 4-H), 1.28, 1.25 (each s, each 3H, $C_5(CH_3)_4$), 1.01 (m, 1H, 4-H′), 0.95 (s, 9H, C$(CH_3)_3$), 0.50, 0.37 (each s, each 3H, Si$(CH_3)_2$). ^{13}C NMR (150.8 MHz, C_6D_6, 298 K): δ = 148.8 (d, $^1J_{CF}$ = 240 Hz, *o*-B$(C_6F_5)_3$), 139.4 (d, $^1J_{CF}$ = 250 Hz, *p*-B$(C_6F_5)_3$), 137.5 (d, $^1J_{CF}$ = 250 Hz, *m*-B$(C_6F_5)_3$), 136.6 (CH, C-2), 134.4 (double intensity), 131.8, 130.2 (each C, α- and *β*-$\underline{C}_5(CH_3)_4$), 106.9 (CH, C-3), 105.0 (C, ipso-$\underline{C}_5(CH_3)_4$), 62.9 (CH_2, C-1), 57.3 (C, $\underline{C}(CH_3)_3$), 34.8 (CH_3, C$(\underline{C}H_3)_3$), ∼31 (CH_2, C-4), 14.9, 12.8, 11.6, 10.0 (each CH_3, α- and *β*-$\underline{C}_5(\underline{C}H_3)_4$), 7.2, 6.7 (each CH_3, Si$(CH_3)_2$), resonance of the ipso-C of B$(C_6F_5)_3$ not detected, resonance of C-4 only detected in the GHSQC spectrum. ^{19}F NMR (564.3 MHz, toluene-d_8, 273 K): δ = −165.5 (broad dd, 2× $^3J_{FF}$ = 20 Hz, 6F, *m*-F), −160.6 (t, $^3J_{FF}$ = 20 Hz, 3F, *p*-F), −135.0 (broad, 6F, *o*-F).

Polymerization Reactions. A 1 L glass autoclave was charged with toluene (300 mL) and triisobutylaluminum (0.5 mL). The mixture was stirred (800 rpm), thermostated and saturated with the gaseous monomer. The polymerization reaction was started by the injection of a toluene solution of the respective betaine complex. After a given time the reaction was stopped by the addition of methanol (15 mL) acidified with HCl (aqueous, 2 N, 15 mL). Polyethylene was precipitated by further addition of aqueous HCl (6 N, 100 mL), collected by fitration, washed with 6 N HCl (50 mL), water (200 mL) and acetone (20 mL) and dried in vacuo to constant weight. Polypropylene was isolated by extraction of the aqueous phase with toluene (50 mL), washing the combined toluene phases with 2 N HCl (200 mL) and water (200 mL), drying over $MgSO_4$ and removal of the solvent in vacuo. Melting points were determined by differential scanning calorimetry using a heating rate of 10 °C/min. The results of the second scan after complete melting and cooling of the samples are reported. The ^{13}C NMR spectrum of the polypropylene sample was recorded on a Bruker AC 200 P spectrometer (^{13}C: 50.3 MHz) with proton decoupling at 350 K in a solvent mixture of 1,2,4-trichlorobenzene and C_6D_6 (5:1).

Polymerization with Betaine 6. Complex **6** was generated in situ as decribed above using 13 mg (39.2 μmol) of butadiene complex **4** and 21 mg (41.0 μmol) of B$(C_6F_5)_3$. Polymerization of ethene: T = 40 °C, reaction time: 5 min, p(ethene) = 2 bar, yield: 10.16 g, activity: 1554 kg PE·mol $[Zr]^{-1}$·h^{-1}·bar^{-1}, melting point: 125 °C. Polymerization of propene: T = 40 °C, reaction time: 60 min, p(propene) = 2 bar, yield: 2.95 g, activity: 38 kg PP·mol $[Zr]^{-1}$·h^{-1}·bar^{-1}, [*mmmm*] = 2.5%, [*mmmr*] = 9.6%, [*rmmr*] = 7.9%, [*mmrr*] = 11.3%, [*mmrm*] + [*rmrr*] = 27.7%, [*rmrm*] = 14.5%, [*rrrr*] = 8.6%, [*mrrr*] = 12.7%, [*mrrm*] = 5.2%.

Polymerization with Betaine 11. The **11A/11B** complex mixture was generated in situ as decribed above using 22 mg (55.7 μmol) of butadiene complex **10** and 29 mg (56.6 μmol) of B$(C_6F_5)_3$. Polymerization of ethene: T = 90 °C, reaction time: 60 min, p(ethene) = 2 bar, yield: 3.12 g, activity: 28 kg PE·mol $[Zr]^{-1}$·h^{-1}·bar^{-1}.

Stoichiometric Reaction of the (Butadiene)zirconium/B(C$_6$F$_5$)$_3$ Betaines with Alkenes, General Procedure. An NMR tube containing a solution of the respective betaine complex in toluene-d_8, prepared in situ as described above, was placed in a Schlenk flask and cooled to −30 °C. While keeping the NMR tube under an argon atmosphere, 4 mL of gaseous 1-alkene (ethene, propene, 1-butene), 3 mL of olefin vapor (1-pentene), or ∼0.02 mL of liquid 1-alkene (1-hexene, 1,5-hexadiene) was slowly bubbled through the solution by a capillary. The tube was then sealed and kept at −20 °C until the NMR spectra were recorded. For the reaction of **11A/11B** with propene, 1-butene, 1-pentene, and 1-hexene the reaction mixture was kept at −20 °C for 8 h prior to the NMR studies.

The following atom-numbering scheme was used below: ring carbon C1 (at Zr) − C6 (attached to B), followed by C7 (substituent at C2) − C10 (in case of the 1-hexene and 1,5-hexadiene insertion products).

Reaction of 6 with ethene, formation of 9a: ^{1}H NMR (599.9 MHz, toluene-d_8, 253 K): δ = 6.10 (1H), 5.87 (2H) (each m, C_5H_4), 5.84 (m, 1H, 4-H), 5.77 (m, 1H, C_5H_4), 5.71 (m, 1H, 5-H), 5.44, 5.16, 4.33, 4.30 (each m, each 1H, C_5H_4), 1.93 (m, 1H, 2-H), 1.59 (m, 1H, 2-H′), 1.41 (m, 1H, 3-H), 1.00 (m, 1H, 3-H′), 0.92 (m, 1H, 1-H), 0.72 (broad s, 1H, 6-H), 0.25 (broad s, 1H, 6-H′), 0.02, −0.20 (each s, each 3H, Si$(CH_3)_2$), −0.23 (m, 1H, 1-H′). ^{13}C NMR (150.8 MHz, toluene-d_8, 253 K): δ = 148.4 (d, $^1J_{CF}$ = 240 Hz, *o*-B$(C_6F_5)_3$), 143.5 (CH, C-4), 139.1 (d, $^1J_{CF}$ = 250 Hz, *p*-B$(C_6F_5)_3$), 137.4 (d, $^1J_{CF}$ = 250 Hz, *m*-B$(C_6F_5)_3$), ∼125 (CH, under solvent signal, C-5), 124.7, 120.3, 118.6, 118.5, 112.7, 112.5, 107.4, 105.5 (each CH, α- and *β*-C_5H_4), 103.0, 101.9 (each C, ipso-C_5H_4), 48.7 (CH_2, C-1), 42.6 (CH_2, C-2), 34.6 (CH_2, C-3), ∼4 (CH_2, C-6), −6.4, −6.7 (each CH_3, Si$(CH_3)_2$), resonance of the ipso-C of B$(C_6F_5)_3$ not detected, resonance of C-6 only detected in the GHSQC spectrum. ^{19}F NMR (564.3 MHz, toluene-d_8, 253 K): δ = −165.6 (dd, 2× $^3J_{FF}$ = 21 Hz, 6F, *m*-F), −160.5 (t, $^3J_{FF}$ = 21 Hz, 3F, *p*-F), −133.7 (d, $^3J_{FF}$ = 21 Hz, 6F, *o*-F).

Reaction of 6 with propene, formation of 9b: ^{1}H NMR (599.9 MHz, toluene-d_8, 253 K): δ = 6.12, 5.90, 5.86, 5.77 (each m, each 1H, C_5H_4), 5.64 (m, 2H, 4-H, 5-H), 5.46, 5.15, 4.34, 4.23 (each m, each 1H, C_5H_4), 1.74 (m, 1H, 2-H), 1.43 (m, 1H, 3-H), 0.92 (dd, ^2J = 13.0 Hz, ^3J = 13.0 Hz, 1H, 1-H), 0.72 (broad s, 1H, 6-H), 0.66 (d, ^3J = 6.2 Hz, 3H, 7-H), 0.65 (m, 1H, 3-H′), 0.18 (broad s, 1H, 6-H′), 0.02, −0.21 (each s, each 3H, Si$(CH_3)_2$), −0.51 (ddd, ^2J = 13.0 Hz, 2× ^3J = 1.9 Hz, 1H, 1-H′). ^{13}C NMR (150.8 MHz, toluene-d_8, 253 K): δ = 148.4 (d, $^1J_{CF}$ = 240 Hz, *o*-B$(C_6F_5)_3$), 140.3 (CH, C-4), 139.2 (d, $^1J_{CF}$ = 250 Hz, *p*-B$(C_6F_5)_3$), 137.4 (d, $^1J_{CF}$ = 250 Hz, *m*-B$(C_6F_5)_3$), ∼125 (CH, under solvent signal, α- or *β*-C_4H_5), 123.9 (CH, C-5), 119.7, 118.8, 118.2, 112.6, 112.1, 107.3, 105.6 (each CH, α- and *β*-C_4H_5),

103.0, 102.1 (each C, ipso-C_4H_5), 58.3 (CH_2, C-1), 50.4 (CH, C-2), 42.6 (CH_2, C-3), 27.4 (CH_3, C-7), ~4 (CH_2, C-6), −6.4, −6.7 (each CH_3, $Si(CH_3)_2$), resonance of the ipso-C of $B(C_6F_5)_3$ not detected, resonance of C-6 only detected in the GHSQC spectrum. ^{19}F NMR (564.3 MHz, toluene-d_8, 253 K): $\delta = -165.6$ (dd, $2\times\ ^3J_{FF} = 21$ Hz, 6F, *m*-F), −160.5 (t, $^3J_{FF} = 21$ Hz, 3F, *p*-F), −133.7 (d, $^3J_{FF} = 21$ Hz, 6F, *o*-F).

Reaction of 6 with 1-butene, formation of 9c: ^{1}H NMR (599.9 MHz, toluene-d_8, 253 K): $\delta = 6.05$, 5.94, 5.89, 5.75 (each m, each 1H, C_5H_4), 5.74 (dd, $^3J = 16.0$ Hz, $^3J = 11.8$ Hz, 1H, 4-H), 5.64 (dd, $^3J = 16.0$ Hz, $^3J = 11.6$ Hz, 1H, 5-H), 5.47, 5.21, 4.41, 4.24 (each m, each 1H, C_5H_4), 1.56 (m, 2H, 2-H and 3-H), 0.98 (m, 1H, 7-H), 0.82 (m, 2H, 1-H and 7-H′), 0.70 (dd, $2\times\ ^3J = 7.5$ Hz, 3H, 8-H), 0.67 (ddd, $^2J = 11.8$ Hz, $2\times\ ^3J = 11.8$ Hz, 1H, 3-H′), 0.61 (broad s, 1H, 6-H), 0.30 (broad d, $J = 11.6$ Hz, 1H, 6-H′), 0.03, −0.19 (each s, each 3H, $Si(CH_3)_2$), −0.36 (d, $^2J = 13.1$ Hz, 1H, 1-H′) ppm. ^{13}C NMR (150.8 MHz, toluene-d_8, 253 K): $\delta = 148.4$ (d, $^1J_{CF} = 240$ Hz, *o*-$B(C_6F_5)_3$), 140.5 (CH, C-4), 139.2 (d, $^1J_{CF} = 250$ Hz, *p*-$B(C_6F_5)_3$), 137.4 (d, $^1J_{CF} = 250$ Hz, *m*-$B(C_6F_5)_3$), 125.8 (α- or β-C_5H_4), 123.9 (CH, C-5), 120.2, 118.3, 118.2, 112.6, 112.0, 107.5, 105.8 (each CH, α- and β-C_5H_4), 103.1, 102.3 (each C, ipso-C_5H_4), 57.3 (CH, C-2), 54.6 (CH_2, C-1), 40.7 (CH_2, C-3), 34.5 (CH_2, C-7), 12.3 (CH_3, C-8), ~4 (CH_2, C-6), −6.4, −6.7 (each CH_3, $Si(CH_3)_2$), resonance of the ipso-C of $B(C_6F_5)_3$ not detected, resonance of C-6 only detected in the GHSQC spectrum. ^{19}F NMR (564.3 MHz, toluene-d_8, 253 K): $\delta = -165.5$ (dd, $2\times\ ^3J_{FF} = 21$ Hz, 6F, *m*-F), −160.4 (t, $^3J_{FF} = 21$ Hz, 3F, *p*-F), −133.5 (d, $^3J_{FF} = 21$ Hz, 6F, *o*-F).

Reaction of 6 with 1-pentene, formation of 9d: ^{1}H NMR (599.9 MHz, toluene-d_8, 253 K): $\delta = 6.06$, 6.00, 5.89, 5.78 (each m, each 1H, C_5H_4), 5.76 (m, 1H, 4-H), 5.65 (under monomer signal, 1H, 5-H), 5.47, 5.21, 4.45, 4.27 (each m, each 1H, C_5H_4), 1.69 (m, 1H, 2-H), 1.54 (m, 1H, 3-H), 1.11 (m, 1H, 8-H), 0.96 (m, 1H, 8-H′), 0.89 (dd, $2\times\ ^3J = 7.0$ Hz, 3H, 9-H), 0.88 (m, 1H, 7-H), 0.83 (m, 1H, 1-H), 0.77 (m, 1H, 7-H′), 0.67 (ddd, $^2J = 11.6$ Hz, $2\times\ ^3J = 11.6$ Hz, 1H, 3-H′), 0.61 (broad s, 1H, 6-H), 0.30 (broad m, 1H, 6-H′), 0.03, −0.19 (each s, each 3H, $Si(CH_3)_2$), −0.36 (d, $^2J = 13.3$ Hz, 1H, 1-H′). ^{13}C NMR (150.8 MHz, toluene-d_8, 253 K): $\delta = 148.4$ (d, $^1J_{CF} = 240$ Hz, *o*-$B(C_6F_5)_3$), 140.6 (CH, C-4), 139.2 (d, $^1J_{CF} = 250$ Hz, *p*-$B(C_6F_5)_3$), 137.4 (d, $^1J_{CF} = 250$ Hz, *m*-$B(C_6F_5)_3$), 125.7 (CH, α- or β-C_5H_4), 123.5 (CH, C-5), 120.0, 118.4, 118.3, 112.6, 112.1, 107.5, 105.8 (each CH, α- and β-C_5H_4), 103.1, 102.2 (each C, ipso-C_5H_4), 55.6 (CH, C-2), 55.0 (CH_2, C-1), 43.4 (CH_2, C-7), 41.1 (CH_2, C-3), 21.1 (CH_2, C-8), 14.7 (CH_3, C-9), ~4 (CH_2, C-6), −6.4, −6.7 (each CH_3, $Si(CH_3)_2$), resonance of the ipso-C of $B(C_6F_5)_3$ not detected, resonance of C-6 only detected in the GHSQC spectrum. ^{19}F NMR (564.3 MHz, toluene-d_8, 253 K): $\delta = -165.5$ (dd, $2\times\ ^3J_{FF} = 21$ Hz, 6F, *o*-F), −160.4 (t, $^3J_{FF} = 21$ Hz, 3F, *p*-F), −133.5 (d, $^3J_{FF} = 21$ Hz, 6F, *o*-F).

Reaction of 6 with 1-hexene, formation of 9e: ^{1}H NMR (599.9 MHz, toluene-d_8, 253 K): $\delta = 6.07$, 6.01, 5.91 (each m, each 1H, C_5H_4), 5.79 (ddd, $^3J = 16.0$ Hz, $^3J = 11.6$ Hz, $^3J = 4.1$ Hz, 1H, 4-H), 5.78 (m, 1H, C_5H_4), 5.68 (under monomer signal, m, 5-H), 5.48, 5.22, 4.45, 4.28 (each m, each 1H, C_5H_4), 1.68 (m, 1H, 2-H), 1.56 (m, 1H, 3-H), 1.26 (m, 2H, 9-H and 9-H′), 1.08 (m, 1H, 8-H), 0.96 (dd, $2\times\ ^3J = 7.3$ Hz, 3H, 10-H), 0.94 (m, 2H, 7-H and 8-H′), 0.87 (dd, $^2J = 13.0$ Hz, $^3J = 13.0$ Hz, 1H, 1-H), 0.80 (under monomer signal, m, 1H, 7-H′), 0.69 (ddd, $^2J = 11.6$ Hz, $2\times\ ^3J = 11.6$ Hz, 1H, 3-H′), 0.63 (broad s, 1H, 6-H), 0.31 (broad d, $J = 8.4$ Hz, 1H, 6-H′), 0.04, −0.18 (each s, each 3H, $Si(CH_3)_2$), −0.32 (d, $^2J = 13.0$ Hz, 1H, 1-H′). ^{13}C NMR (150.8 MHz, toluene-d_8, 253 K): $\delta = 148.4$ (d, $^1J_{CF} = 240$ Hz, *o*-$B(C_6F_5)_3$), 140.5 (CH, C-4), 139.2 (d, $^1J_{CF} = 250$ Hz, *p*-$B(C_6F_5)_3$), 137.4 (d, $^1J_{CF} = 250$ Hz, *m*-$B(C_6F_5)_3$), 125.9 (CH, α- or β-C_5H_4), 124.0 (CH, C-5), 120.1, 118.3, 118.2, 112.5, 112.0, 107.5, 105.9 (each CH, α- and β-C_5H_4), 103.2, 102.3 (each C, ipso-C_5H_4), 55.9 (CH, C-2), 55.2 (CH_2, C-1), 41.9 (CH_2, C-7), 41.2 (CH_2, C-3), 30.3 (CH_2, C-8), 23.6 (CH_2, C-9), 14.5 (CH_3, C-10), ~4 (CH_2, C-6), −6.4, −6.7 (each CH_3, $Si(CH_3)_2$), resonance of the ipso-C of $B(C_6F_5)_3$ not detected, resonance of C-6 only detected in the GHSQC spectrum. ^{19}F NMR (564.3 MHz, toluene-d_8, 253 K): $\delta = -165.6$ (broad dd, $2\times\ ^3J_{FF} = 21$ Hz, 6F, *m*-F), −160.6 (t, $^3J_{FF} = 21$ Hz, 3F, *p*-F), −133.6 (d, $^3J_{FF} = 21$ Hz, 6F, *o*-F).

Reaction of 6 with 1,5-hexadiene, formation of 9f: ^{1}H NMR (599.9 MHz, toluene-d_8, 253 K): $\delta = 6.05$, 6.01, 5.88, 5.77 (each m, each 1H, C_5H_4), 5.73 (m, 1H, 4-H), 5.69 (m, 1H, 9-H), 5.65 (under monomer signal, m, 1H, 5-H), 5.01 (m, 2H, 10-H and 10-H′), 5.47, 5.21, 4.50, 4.26 (each m, each 1H, C_5H_4), 1.83 (m, 1H, 8-H), 1.70 (m, 2H, 2-H and 8-H′), 1.50 (broad d, $^2J = 11.8$ Hz, 1H, 3-H), 1.02 (m, 1H, 7-H), 0.81 (m, 1H, 7-H′), 0.76 (dd, $^2J = 13.0$ Hz, $^3J = 13.0$ Hz, 1H, 1-H), 0.65 (ddd, $^2J = 11.8$ Hz, $2\times\ ^3J = 11.8$ Hz, 1H, 3-H′), 0.61 (broad s, 1H, 6-H), 0.29 (broad s, 1H, 6-H′), 0.04, −0.17 (each s, each 3H, $Si(CH_3)_2$), −0.36 (d, $^2J = 13.1$ Hz, 1H, 1-H′). ^{13}C NMR (150.8 MHz, toluene-d_8, 253 K): $\delta = 148.4$ (d, $^1J_{CF} = 240$ Hz, *o*-$B(C_6F_5)_3$), 140.2 (CH, C-4), 139.2 (d, $^1J_{CF} = 250$ Hz, *p*-$B(C_6F_5)_3$), 138.9 (CH, C-9), 137.4 (d, $^1J_{CF} = 250$ Hz, *m*-$B(C_6F_5)_3$), 125.6 (CH, α- or β-C_5H_4), 124.0 (CH, C-5), 120.0, 118.4, 118.2 (each CH, α- and β-C_5H_4), 114.7 (CH_2, C-10), 112.6, 112.1, 107.5, 105.8 (each CH, α- or β-C_5H_4), 103.1, 102.2 (each C, ipso-C_5H_4), 54.7 (CH, C-2), 54.1 (CH_2, C-1), 41.1 (CH_2, C-3), 40.2 (CH_2, C-7), 32.1 (CH_2, C-8), ~4 (CH_2, C-6), −6.4, −6.7 (each CH_3, $Si(CH_3)_2$), resonance of the ipso-C of $B(C_6F_5)_3$ not detected, resonance of C-6 only detected in the GHSQC spectrum. ^{19}F NMR (564.3 MHz, toluene-d_8, 253 K): $\delta = -165.6$ (broad dd, $2\times\ ^3J_{FF} = 21$ Hz, 6F, *m*-F), −160.4 (t, $^3J_{FF} = 21$ Hz, 3F, *p*-F), −133.6 (d, $^3J_{FF} = 21$ Hz, 6F, *o*-F).

Reaction of 11 with ethene, formation of 14a: ^{1}H NMR (599.9 MHz, toluene-d_8, 253 K): $\delta = 5.04$ (m, 1H, 5-H), 4.95 (ddd, $2\times\ ^3J = 12.0$ Hz, $^3J = 4.8$ Hz, 1H, 4-H), 2.03 (broad d, $^2J = 13.8$ Hz, 1H, 6-H), 2.01 (s, 3H, $C_5(CH_3)_4$), 1.77 (broad s, 1H, 6-H′), 1.64 (m, 1H, 2-H), 1.57, 1.55, 1.51 (each s, each 3H, $C_5(CH_3)_4$), 1.37 (ddd, $3\times\ ^3J = 12.0$ Hz, 1H, 3-H), 0.93 (s, 9H, $C(CH_3)_3$), 0.92 (m, 1H, 2-H′), 0.82 (m, 1H, 1-H), 0.75 (m, 1H, 3-H′), 0.54 (ddd, $^2J = 13.7$ Hz, $^3J = 11.9$ Hz, $^3J = 7.2$ Hz, 1H, 1-H′), 0.44, 0.23 (each s, each 3H, $Si(CH_3)_2$). ^{13}C NMR (150.8 MHz, toluene-d_8, 253 K): $\delta = 149.8$ (CH, C-4), 148.4 (d, $^1J_{CF} = 250$ Hz, *o*-$B(C_6F_5)_3$), 139.2 (d, $^1J_{CF} = 250$ Hz, *p*-$B(C_6F_5)_3$), 137.3 (d, $^1J_{CF} = 250$ Hz, *m*-$B(C_6F_5)_3$), 130.6, 129.4 (each C, α- and β-$\underline{C}_5(CH_3)_4$), 125.8 (CH, C-5), 102.1 (C, ipso-$\underline{C}_5(CH_3)_4$), 61.5 (CH_2, C-1), 57.7 (C, $\underline{C}(CH_3)_3$), 34.3 (CH_2, C-2), 33.1 (CH_3, triple intensity, $C(CH_3)_3$), 32.1 (CH_2, C-6), 29.7 (CH_2, C-3), 16.1, 13.1, 11.4, 11.3 (each CH_3, $C_5(\underline{C}H_3)_4$), 6.5, 5.7 (each CH_3, $Si(CH_3)_2$), resonance of the ipso-C of $B(C_6F_5)_3$ not detected.

Reaction of 11 with propene, formation of 14b: ^{1}H NMR (599.9 MHz, toluene-d_8, 253 K): $\delta = 5.07$ (ddd, $^3J = 15.0$ Hz, $^3J = 11.6$ Hz, $^3J = 4.6$ Hz, 1H, 5-H), 4.95 (m, 1H, 4-H), 2.05 (broad d, $^2J = 13.8$ Hz, 1H, 6-H), 2.01 (s, 3H, $C_5(CH_3)_4$), 1.81 (broad s, 1H, 6-H′), 1.60, 1.57, 1.54 (each s, each 3H, $C_5(CH_3)_4$), 1.28 (m, 2H, 2-H and 3-H), 0.98 (m, 1H, 1-H), 0.94 (s, 9H, $C(CH_3)_3$), 0.67 (m, 1H, 3-H′), 0.62 (d, $^3J = 5.6$ Hz, 3H, 7-H), 0.44 (s, 3H, $Si(CH_3)_2$), 0.42 (m, 1H, 1-H′), 0.24 (s, 3H, $Si(CH_3)_2$). ^{13}C NMR (150.8 MHz, toluene-d_8, 253 K): $\delta = 148.4$ (d, $^1J_{CF} = 250$ Hz, *o*-$B(C_6F_5)_3$), 147.5 (CH, C-4), 139.4 (d, $^1J_{CF} = 250$ Hz, *p*-$B(C_6F_5)_3$), 137.3 (d, $^1J_{CF} = 250$ Hz, *m*-$B(C_6F_5)_3$), 135.1, 133.1, 130.6, 129.5 (each C, α- and β-$\underline{C}_5(CH_3)_4$), 125.8 (CH, C-5), 102.1 (C, ipso-$\underline{C}_5(CH_3)_4$), 71.2 (CH_2, C-1), 57.6 (C, $\underline{C}(CH_3)_3$), 39.9 (CH, C-2), 37.2 (CH_2, C-3), 32.5 (CH_3, triple intensity, $C(\underline{C}H_3)_3$), 27.5 (CH_3, C-7), 16.2, 13.1, 11.6, 11.4 (each CH_3, $C_5(\underline{C}H_3)_4$), 6.5, 5.7 (each CH_3, $Si(CH_3)_2$), resonances of the ipso-C of $B(C_6F_5)_3$ and of C-6 not detected.

Reaction of 11 with 1-butene, formation of 14c: ^{1}H NMR (599.9 MHz, toluene-d_8, 253 K): $\delta = 5.10$ (ddd, $^3J = 14.6$ Hz, $^3J = 11.5$ Hz, $^3J = 4.3$ Hz, 1H, 5-H), 4.92 (ddd, $2\times\ ^3J = 11.5$ Hz, $^3J = 4.3$ Hz, 1H, 4-H), 2.03 (under solvent signal, 1H, 6-H), 2.02 (s, 3H, $C_5(CH_3)_4$), 1.83 (broad s, 1H, 6-H′), 1.62, 1.59, 1.55 (each s, each 3H, $C_5(CH_3)_4$), 1.28 (ddd, $^2J = 12.6$ Hz, $2\times\ ^3J = 12.6$ Hz, 1H, 3-H), 1.03 (m, 1H, 2-H), 1.00 (m, 1H, 1-H), 0.94 (s, 9H, $C(CH_3)_3$), 0.89, 0.80 (each m, each 1H, 7-H, 7-H′), 0.73 (m, 1H, 3-H′), 0.62 (dd, $2\times\ ^3J = 7.3$ Hz, 3H, 8-H), 0.44 (s, 3H, $Si(CH_3)_2$), 0.32 (dd, $^2J = 13.4$ Hz, $^3J = 10.8$ Hz, 1H, 1-H′), 0.25 (s, 3H, $Si(CH_3)_2$). ^{13}C NMR (150.8 MHz, toluene-d_8, 253 K): $\delta = 148.4$ (d, $^1J_{CF} = 240$ Hz, *o*-$B(C_6F_5)_3$), 147.2 (CH, C-4), 139.4 (d, $^1J_{CF} = 250$ Hz, *p*-$B(C_6F_5)_3$), 137.3 (d, $^1J_{CF} = 250$ Hz, *m*-$B(C_6F_5)_3$), 135.1, 133.3, 130.6, 129.5 (each C, α- and β-$\underline{C}_5(CH_3)_4$), 126.1 (CH, C-5), 102.1 (C, ipso-$\underline{C}_5(CH_3)_4$), 66.9 (CH_2, C-1), 57.6 (C, $\underline{C}(CH_3)_3$), 45.6 (CH, C-2), 35.0 ($\underline{C}H_2$, C-3), 33.8 (CH_2, C-7), 33.1 (CH_3, triple intensity, $C(\underline{C}H_3)_3$), ~31 (CH_2, C-6), 16.2, 13.2, 11.6, 11.4 (each CH_3, $C_5(\underline{C}H_3)_4$), 10.9 (CH_3, C-8), 6.5, 5.7 (each CH_3, $Si(CH_3)_2$),

resonance of the ipso-C of $B(C_6F_5)_3$ not detected, resonance of C-6 only detected in the GHSQC spectrum. ^{19}F NMR (564.3 MHz, toluene-d_8, 253 K): $\delta = -165.6$ (broad, 6F, *m*-F), -160.6 (t, $^3J_{FF} = 21$ Hz, 3F, *p*-F), -133.5 (broad, 6F, *o*-F).

Reaction of 11 with 1-pentene, formation of 14d: ^1H NMR (599.9 MHz, toluene-d_8, 253 K): $\delta = 5.09$ (ddd, $^3J = 14.5$ Hz, $^3J = 11.5$ Hz, $^3J = 4.7$ Hz, 1H, 5-H), 4.98 (m, 1H, 4-H), 2.05 (broad d, $^3J = 14.5$ Hz, 1H, 6-H), 2.01 (s, 3H, $C_5(CH_3)_4$), 1.82 (broad s, 1H, 6-H′), 1.63, 1.62, 1.59 (each s, each 3H, $C_5(CH_3)_4$), 1.30 (ddd, $^2J = 12.7$ Hz, $2\times$ $^3J = 12.7$ Hz, 1H, 3-H), 1.14 (m, 1H, 2-H), 1.06 (m, 1H, 8-H), 1.04 (m, 1H, 1-H), 0.97 (m, 1H, 8-H′), 0.88, 0.78 (each m, each 1H, 7-H, 7-H′), 0.94 (s, 9H, $C(CH_3)_3$), 0.76 (under monomer signal, 1H, 3-H′), 0.74 (dd, $2\times$ $^3J = 7.1$ Hz, 3H, 9-H), 0.44 (s, 3H, $Si(CH_3)_2$), 0.31 (dd, $^2J = 13.6$ Hz, $^3J = 11.0$ Hz, 1H, 1-H′), 0.26 (s, 3H, $Si(CH_3)_2$). ^{13}C NMR (150.8 MHz, toluene-d_8, 253 K): $\delta = 148.4$ (d, $^1J_{CF} = 240$ Hz, *o*-$B(C_6F_5)_3$), 147.3 (CH, C-4), 139.4 (d, $^1J_{CF} = 250$ Hz, *p*-$B(C_6F_5)_3$), 137.3 (d, $^1J_{CF} = 250$ Hz, *m*-$B(C_6F_5)_3$), 135.1, 133.3, 130.6, 129.5 (each C, α- and *β*-$\underline{C}_5(CH_3)_4$), 126.0 (CH, C-5), 102.2 (C, ipso-$\underline{C}_5(CH_3)_4$), 67.6 (CH_2, C-1), 57.6 (C, $\underline{C}(CH_3)_3$), 43.9 (CH, C-2), 43.3 ($\overline{CH}_2$, C-7), 35.7 (CH_2, C-3), 33.2 ($\overline{CH}_3$, triple intensity, $C(\underline{C}H_3)_3$), ∼31 (CH_2, C-6), 20.0 (CH_2, C-8), 16.2, 14.0 (each CH_3, $C_5(\underline{C}H_3)_4$), 13.1 (CH_3, C-9), 11.6, 11.4 (each CH_3, $C_5(\underline{C}H_3)_4$), 6.5, 5.7 (each CH_3, $Si(CH_3)_2$), resonance of the ipso-C of $B(C_6F_5)_3$ not detected, resonance of C-6 only detected in the GHSQC spectrum. ^{19}F NMR (564.3 MHz, toluene-d_8, 253 K): $\delta = -165.7$ (broad, 6F, *m*-F), -160.7 (t, $^3J_{FF} = 21$ Hz, 3F, *p*-F), -133.6 (broad, 6F, *o*-F).

Reaction of 11 with 1-hexene, formation of 14e: ^1H NMR (599.9 MHz, toluene-d_8, 253 K): $\delta = 5.10$ (m, 1H, 5-H), 5.00 (ddd, $2\times$ $^3J = 12.0$ Hz, $^3J = 4.5$ Hz, 1H, 4-H), 2.04 (broad s, 1H, 6-H), 2.01 (s, 3H, $C_5(CH_3)_4$), 1.82 (broad s, 1H, 6-H′), 1.63, 1.61, 1.60 (each s, each 3H, $C_5(CH_3)_4$), 1.31 (ddd, $^2J = 12.6$ Hz, $2\times$ $^3J = 12.0$ Hz, 1H, 3-H), 1.16 (under monomer signal, 3H, 2-H, 9-H, 9-H′), 1.08 (m, 1H, 1-H), 1.04 (m, 1H, 8-H), 0.95 (m, 2H, 7-H, 8-H′), 0.94 (s, 9H, $C(CH_3)_3$), 0.86 (dd, $2\times$ $^3J = 7.2$ Hz, 3H, 10-H), 0.83 (m, 1H, 7-H′), 0.78 (m, 1H, 3-H′), 0.44 (s, 3H, $Si(CH_3)_2$), 0.35 (dd, $^2J = 13.7$ Hz, $^3J = 11.2$ Hz, 1H, 1-H′), 0.26 (s, 3H, $Si(CH_3)_2$). ^{13}C NMR (150.8 MHz, toluene-d_8, 253 K): $\delta = 148.4$ (d, $^1J_{CF} = 240$ Hz, *o*-$B(C_6F_5)_3$), 147.3 (CH, C-4), 139.4 (d, $^1J_{CF} = 250$ Hz, *p*-$B(C_6F_5)_3$), 137.3 (d, $^1J_{CF} = 250$ Hz, *m*-$B(C_6F_5)_3$), 135.2, 133.3, 130.6, 129.6 (each C, α- and *β*-$\underline{C}_5(CH_3)_4$), 126.1 (CH, C-5), 121.6 (C, ipso-$B(C_6F_5)_3$), 102.2 (C, ipso-$\underline{C}_5(CH_3)_4$), 67.7 (CH_2, C-1), 57.6 (C, $\underline{C}(CH_3)_3$), 44.2 (CH, C-2), 41.0 ($\overline{CH}_2$, C-7), 35.7 (CH_2, C-3), 33.2 ($\overline{CH}_3$, triple intensity, $C(\underline{C}H_3)_3$), 29.2 (CH_2, C-8), 23.0 (CH_2, C-9), 16.2 (CH_3, $C_5(\underline{C}H_3)_4$), 14.4 ($\overline{CH}_3$, double intensity, C-10 and $C_5(\underline{C}H_3)_4$), 11.7, 11.4 (each CH_3, $C_5(\underline{C}H_3)_4$), 6.5, 5.7 (each CH_3, $Si(CH_3)_2$), resonance of C-6 not detected. ^{19}F NMR (564.3 MHz, toluene-d_8, 253 K): $\delta = -165.7$ (broad, 6F, *m*-F), -160.7 (t, $^3J_{FF} = 21$ Hz, 3F, *p*-F), -133.5 (broad, 6F, *o*-F).

Reaction of 11 with 1,5-hexadiene, formation of 14f: ^1H NMR (599.9 MHz, toluene-d_8, 253 K): $\delta = 5.51$ (m, 1H, 9-H), 5.05 (ddd, $^3J = 14.3$ Hz, $^3J = 10.5$ Hz, $^3J = 4.5$ Hz, 1H, 5-H), 4.96 (under monomer signal, 3H, 4-H, 10-H, 10-H′), 2.02 (broad d, $^3J = 14.3$ Hz, 1H, 6-H), 2.00 (s, 3H, $C_5(CH_3)_4$), 1.82 (broad s, 1H, 6-H′), 1.78 (m, 1H, 8-H), 1.66 (m, 1H, 8-H′), 1.62, 1.61, 1.60 (each s, each 3H, $C_5(CH_3)_4$), 1.26 (ddd, $3\times$ $^3J = 12.5$ Hz, 1H, 3-H), 1.13 (m, 1H, 2-H), 1.03 (m, 1H, 1-H), 0.96 (m, 1H, 7-H), 0.93 (s, 9H, $C(CH_3)_3$), 0.75 (m, 1H, 7-H′), 0.69 (m, 1H, 3-H′), 0.43, 0.26 (each s, each 3H, $Si(CH_3)_2$), 0.20 (m, 1H, 1-H′). ^{13}C NMR (150.8 MHz, toluene-d_8, 253 K): $\delta = 148.4$ (d, $^1J_{CF} = 240$ Hz, *o*-$B(C_6F_5)_3$), 147.2 (CH, C-4), 139.4 (d, $^1J_{CF} = 250$ Hz, *p*-$B(C_6F_5)_3$), 138.6 (CH, C-9), 137.3 (d, $^1J_{CF} = 250$ Hz, m-$B(C_6F_5)_3$), 135.1, 133.4, 130.7, 129.6 (each C, α- and *β*-$\underline{C}_5(CH_3)_4$), 125.9 (CH, C-5), 114.6 (CH_2, C-10), 102.2 (C, ipso-$\underline{C}_5(CH_3)_4$), 66.6 (CH_2, C-1), 57.6 (C, $\underline{C}(CH_3)_3$), 43.1 (CH, C-2), 39.7 ($\overline{CH}_2$, C-7), 35.9 (CH_2, C-3), 33.2 (CH_3, triple intensity, $C(\underline{C}H_3)_3$), 31.2 (CH_2, C-8), 16.3, 13.1, 11.8, 11.4 (each CH_3, $C_5(\underline{C}H_3)_4$), 6.5, 5.7 (each CH_3, $Si(CH_3)_2$), resonances of the ipso-C of $B(\underline{C}_6F_5)_3$ and of C-6 not detected. ^{19}F NMR (564.3 MHz, toluene-d_8, 253 K): $\delta = -165.6$ (broad, 6F, *m*-F), -160.6 (t, $^3J_{FF} = 21$ Hz, 3F, *p*-F), -133.6 (broad, 6F, *o*-F). ^{19}F NMR (564.3 MHz, toluene-d_8, 193 K): $\delta = -167.0$, -165.9, -165.4, -164.8, -164.4, -163.0 (each broad, each 1F, *m*-F), -160.4, -159.8, -159.3 (each broad, each 1F, *p*-F), -141.4, -135.2, -133.5, -133.3 (each 1F), -129.8 (2F) (each br, *o*-F).

Kinetic Investigation of the 1-Alkene Insertion into the Zr−C Bond of the Betaines 6 and 11. General procedure. A solution of the respective betaine complex was prepared in situ using toluene-d_8 containing an accurate internal ferrocene standard (c(Fc) between 0.02 and 0.03 mol/L). According to the general procedure described above, 10 mL of gaseous or 0.05 mL of liquid 1-alkene were injected into the solution at −60 °C. The sample was immediately brought inside the NMR spectrometer and warmed there to the respective reaction temperature. The overall chemical reaction rate was measured by recording one scan (^1H) each minute for a period of ∼40 min. The 1-alkene concentration was determined by integration of one separated olefin signal versus the internal ferrocene standard.

Alkene Insertions into the Zr−C Bond of 6. The starting concentration of **6** was ∼8 mmol/L. For the determination of the pseudo-first-order rate constant $k_{c(exp)}(T)$ the decay of the intensities of the $(CH_3)_2Si(C_5H_4)_2$ signals of **6** was monitored. The overall activation energies $\Delta G^{\ddagger}_{chem}$ for the 1-alkene insertion process are calculated from the second-order rate constants $k_{chem} = k_{c(exp)}/c_{alkene}$.

Formation of ***9b***: (1): $T = 243$ K, c(propene) = 0.004 mol/L, $k_{c(exp)} = 1.89\cdot10^{-3}$ s^{-1}, $k_{chem} = 4.30\cdot10^{-1}$ L·(mol·s)$^{-1}$; (2): $T = 243$ K, c(propene) = 0.012 mol/L, $k_{c(exp)} = 2.02\cdot10^{-3}$ s^{-1}, $k_{chem} = 1.68\cdot10^{-1}$ L·(mol·s)$^{-1}$. Average value from run (1) and (2): $k_{chem} = 2.99\cdot10^{-1}$ L·(mol·s)$^{-1}$, $\Delta G^{\ddagger}_{chem} = 14.7 \pm 0.1$ kcal/mol.

Formation of ***9c***: (1): $T = 243$ K, c(1-butene) = 0.026 mol/L, $k_{c(exp)} = 7.71\cdot10^{-3}$ s^{-1}, $k_{chem} = 2.97\cdot10^{-1}$ L·(mol·s)$^{-1}$; (2): $T = 243$ K, c(1-butene) = 0.028 mol/L, $k_{c(exp)} = 4.07\cdot10^{-3}$ s^{-1}, $k_{chem} = 1.45\cdot10^{-1}$ L·(mol·s)$^{-1}$. Average value from run (1) and (2): $k_{chem} = 2.21\cdot10^{-1}$ L·(mol·s)$^{-1}$, $\Delta G^{\ddagger}_{chem} = 14.9 \pm 0.1$ kcal/mol.

Formation of ***9d***: (1): $T = 243$ K, c(1-pentene) = 0.078 mol/L, $k_{c(exp)} = 7.10\cdot10^{-3}$ s^{-1}, $k_{chem} = 9.13\cdot10^{-2}$ L·(mol·s)$^{-1}$; (2): $T = 243$ K, c(1-pentene) = 0.067 mol/L, $k_{c(exp)} = 4.91\cdot10^{-3}$ s^{-1}, $k_{chem} = 7.31\cdot10^{-2}$ L·(mol·s)$^{-1}$. Average value from run (1) and (2): $k_{chem} = 8.22\cdot10^{-2}$ L·(mol·s)$^{-1}$, $\Delta G^{\ddagger}_{chem} = 15.3 \pm 0.1$kcal/mol.

Formation of ***9e***: (1): $T = 243$ K, c(1-hexene) = 0.066 mol/L, $k_{c(exp)} = 3.90\cdot10^{-3}$ s^{-1}, $k_{chem} = 5.91\cdot10^{-2}$ L·(mol·s)$^{-1}$; (2): $T = 243$ K, c(1-hexene) = 0.060 mol/L, $k_{c(exp)} = 2.97\cdot10^{-3}$ s^{-1}, $k_{chem} = 4.95\cdot10^{-2}$ L·(mol·s)$^{-1}$. Average value from run (1) and (2): $k_{chem} = 5.43\cdot10^{-2}$ L·(mol·s)$^{-1}$, $\Delta G^{\ddagger}_{chem} = 15.5 \pm 0.1$ kcal/mol.

Alkene Insertions into the Zr−C Bond of 11A/11B. The starting concentration of **11A** + **11B** was ∼6 mmol/L. For the determination of the pseudo-first-order rate constant $k_{c(exp)}(T)$ the decay of the intensities of the $NC(CH_3)_3$ signals of the two isomeric betaines **11A/11B** was monitored. Under all conditions described below no significant difference in the reactivities of the two isomers was observed. Thus, an averaged rate constant $k_{chem}(T)$ is reported for each kinetic experiment. The overall activation energies $\Delta G^{\ddagger}_{chem}$ for the 1-alkene insertion process are calculated from the second-order rate constants $k_{chem} = k_{c(exp)}/c_{alkene}$.

Formation of ***14a***: (1): $T = 253$ K, c(ethene) = 0.341 mol/L, $k_{c(exp)} = 1.36\cdot10^{-3}$ s^{-1}, $k_{chem} = 3.99\cdot10^{-3}$ L·(mol·s)$^{-1}$; (2): $T = 253$ K, c(ethene) = 0.416 mol/L, $k_{c(exp)} = 2.33\cdot10^{-3}$ s^{-1}, $k_{chem} = 5.60\cdot10^{-3}$ L·(mol·s)$^{-1}$. Average value from run (1) and (2): $k_{chem} = 4.80\cdot10^{-3}$ L·(mol·s)$^{-1}$, $\Delta G^{\ddagger}_{chem} = 17.4 \pm 0.1$ kcal/mol.

Formation of ***14b***: (1): $T = 273$ K, c(propene) = 0.097 mol/L, $k_{c(exp)} = 6.36\cdot10^{-4}$ s^{-1}, $k_{chem} = 6.56\cdot10^{-3}$ L·(mol·s)$^{-1}$; (2): $T = 273$ K, c(propene) = 0.805 mol/L, $k_{c(exp)} = 3.17\cdot10^{-3}$ s^{-1}, $k_{chem} = 3.94\cdot10^{-3}$ L·(mol·s)$^{-1}$. Average value from run (1) and (2): $k_{chem} = 5.22\cdot10^{-3}$ L·(mol·s)$^{-1}$, $\Delta G^{\ddagger}_{chem} = 18.8 \pm 0.1$ kcal/mol.

Formation of ***14c***: (1): $T = 273$ K, c(1-butene) = 0.068 mol/L, $k_{c(exp)} = 2.71\cdot10^{-4}$ s^{-1}, $k_{chem} = 3.99\cdot10^{-3}$ L·(mol·s)$^{-1}$; (2): $T = 273$ K, c(1-butene) = 0.057 mol/L, $k_{c(exp)} = 2.06\cdot10^{-4}$ s^{-1}, $k_{chem} = 3.62\cdot10^{-3}$ L·(mol·s)$^{-1}$. Average value from run (1) and (2): $k_{chem} = 3.80\cdot10^{-3}$ L·(mol·s)$^{-1}$, $\Delta G^{\ddagger}_{chem} = 19.0 \pm 0.1$ kcal/mol.

Formation of ***14d***: (1): $T = 288$ K, c(1-pentene) = 0.127 mol/L, $k_{c(exp)} = 9.92\cdot10^{-4}$ s^{-1}, $k_{chem} = 7.81\cdot10^{-3}$ L·(mol·s)$^{-1}$; (2): $T = 288$ K, c(1-pentene) = 0.268 mol/L, $k_{c(exp)} = 1.00\cdot10^{-3}$ s^{-1}, $k_{chem} = 3.74\cdot10^{-3}$ L·(mol·s)$^{-1}$. Average value from run (1) and (2): $k_{chem} = 5.74\cdot10^{-3}$ L·(mol·s)$^{-1}$, $\Delta G^{\ddagger}_{chem} = 19.8 \pm 0.1$ kcal/mol.

Formation of ***14e***: (1): $T = 293$ K, c(1-hexene) = 0.339 mol/L, $k_{c(exp)} = 1.42\cdot10^{-3}$ s^{-1}, $k_{chem} = 4.19\cdot10^{-3}$ L·(mol·s)$^{-1}$; (2): $T = 293$ K, c(1-hexene) = 1.065 mol/L, $k_{c(exp)} = 2.59\cdot10^{-3}$ s^{-1}, $k_{chem} = 2.42\cdot10^{-3}$

$L\cdot(mol\cdot s)^{-1}$. Average value from run (1) and (2): $k_{chem} = 3.31\cdot10^{-3}$ $L\cdot(mol\cdot s)^{-1}$, $\Delta G^{\ddagger}_{chem} = 20.5 \pm 0.1$ kcal/mol.

Formation of ***14f***: (1): $T = 273$ K, c(1,5-hexadiene) = 0.887 mol/L, $k_{c(exp)} = 2.51\cdot10^{-3}$ s^{-1}, $k_{chem} = 2.83\cdot10^{-3}$ $L\cdot(mol\cdot s)^{-1}$; (2): $T = 273$ K, c(1,5-hexadiene) = 0.663 mol/L, $k_{c(exp)} = 1.91\cdot10^{-3}$ s^{-1}, $k_{chem} = 2.88\cdot10^{-3}$ $L\cdot(mol\cdot s)^{-1}$. Average value from run (1) and (2): $k_{chem} = 2.86\cdot10^{-3}$ $L\cdot(mol\cdot s)^{-1}$; $k_{chem}/2 = 1.43\cdot10^{-3}$ $L\cdot(mol\cdot s)^{-1}$, $\Delta G^{\ddagger}_{chem} = 19.5 \pm 0.1$ kcal/mol.

Kinetic Study of the Allyl Ligand Automerization Process in 6 and 11A/11B, General Procedure. The measurements of the first-order rate constants $k_{m(exp)}$ of the allyl inversion process were performed analogously by using the internal ferrocene standard. The $k_{m(exp)}$ values listed below are averaged values from 6 to 10 measurements at a given temperature and monomer concentration. The $\Delta G^{\ddagger}_{m(obs)}$ values are derived from $k_{m(obs)} = (k_{m(exp)} - k_{m(solv)})/c_{alkene}$. The values for $k_{m(solv)}$ and $\Delta G^{\ddagger}_{m(obs)}$ were determined in the absence of an 1-alkene.

Configurational inversion at the allyl unit in 6: *Pure solvent:* $T = 243$ K, $k_{m(solv)} = 0.352$ s^{-1}, $\Delta G^{\ddagger}_{m(solv)} = 14.6 \pm 0.1$ kcal/mol. *1-Butene*: (1): $T = 243$ K, c(1-butene) = 0.015 mol/L, $k_{m(exp)} = 0.42$ s^{-1}, $k_{m(obs)} = 4.20$ $L\cdot(mol\cdot s)^{-1}$. (2): $T = 243$ K, c(1-butene) = 0.011 mol/L, $k_{m(exp)} = 0.38$ s^{-1}, $k_{m(obs)} = 2.73$ $L\cdot(mol\cdot s)^{-1}$. Average value from run (1) and (2): $k_{m(obs)} = 3.46$ $L\cdot(mol\cdot s)^{-1}$. *1-Pentene:* (1): $T = 243$ K, c(1-pentene) = 0.009 mol/L, $k_{m(exp)} = 0.37$ s^{-1}, $k_{m(obs)} = 1.56$ $L\cdot(mol\cdot s)^{-1}$. (2): $T = 243$ K, c(1-pentene) = 0.039 mol/L, $k_{m(exp)} = 0.52$ s^{-1}, $k_{m(obs)} = 4.18$ $L\cdot(mol\cdot s)^{-1}$. Average value from run (1) and (2): $k_{m(obs)} = 2.87$ $L\cdot(mol\cdot s)^{-1}$. *1-Hexene:* (1): $T = 243$ K, c(1-hexene) = 0.066 mol/L, $k_{m(exp)} = 0.45$ s^{-1}, $k_{m(obs)} = 1.44$ $L\cdot(mol\cdot s)^{-1}$. (2): $T = 243$ K, c(1-hexene) = 0.060 mol/L, $k_{m(exp)} = 0.50$ s^{-1}, $k_{m(obs)} = 2.38$ $L\cdot(mol\cdot s)^{-1}$. Average value from run (1) and (2): $k_{m(obs)} = 1.91$ $L\cdot(mol\cdot s)^{-1}$ (for calculated errors see the Supporting Information).

Configurational inversion at the allyl unit in 11A/11B: *Pure solvent:* (1): $T = 303$ K, $k_{m(solv)} = 1.29$ s^{-1}. (2): $T = 303$ K, $k_{m(solv)} = 1.28$ s^{-1}. Average value from run (1) and (2): $k_{m(solv)} = 1.28$ s^{-1}, $\Delta G^{\ddagger}_{m(solv)} = 17.6 \pm 0.1$ kcal/mol. From the experimental $\Delta G^{\ddagger}_{m(solv)}$ value $k_{m(solv)}$ can be calculated at varying temperatures: $k_{m(solv)}(288\ K) = 0.27$ s^{-1}; $k_{m(solv)}(278\ K) = 0.08$ s^{-1}. *Propene:* (1): $T = 278$ K, c(propene) = 0.378 mol/L, $k_{m(exp)} = 0.25$ s^{-1}, $k_{m(obs)} = 0.44$ $L\cdot(mol\cdot s)^{-1}$. (2): $T = 278$ K, c(propene) = 0.565 mol/L, $k_{m(exp)} = 0.29$ s^{-1}, $k_{m(obs)} = 0.36$ $L\cdot(mol\cdot s)^{-1}$. Average value from run (1) and (2): $k_{m(obs)} = 0.40$ $L\cdot(mol\cdot s)^{-1}$. *1-Butene*: (1): $T = 288$ K, c(1-butene) = 0.282 mol/L, $k_{m(exp)} = 0.50$ s^{-1}, $k_{m(obs)} = 0.84$ $L\cdot(mol\cdot s)^{-1}$. (2): $T = 288$ K, c(1-butene) = 0.322 mol/L, $k_{m(exp)} = 0.62$ s^{-1}, $k_{m(obs)} = 1.11$ $L\cdot(mol\cdot s)^{-1}$. Average value from run (1) and (2): $k_{m(obs)} = 0.97$ $L\cdot(mol\cdot s)^{-1}$. *1-Pentene:* (1): $T = 288$ K, c(1-pentene) = 1.605 mol/L, $k_{m(exp)} = 0.74$ s^{-1}, $k_{m(obs)} = 0.30$ $L\cdot(mol\cdot s)^{-1}$. (2): $T = 288$ K, c(1-pentene) = 0.631 mol/L, $k_{m(exp)} = 0.64$ s^{-1}, $k_{m(obs)} = 0.59$ $L\cdot(mol\cdot s)^{-1}$. (3): $T = 288$ K, c(1-pentene) = 0.617 mol/L, $k_{m(exp)} = 0.40$ s^{-1}, $k_{m(obs)} = 0.22$ $L\cdot(mol\cdot s)^{-1}$. Average value from run (1) to (3): $k_{m(obs)} = 0.37$ $L\cdot(mol\cdot s)^{-1}$. *1-Hexene:* (1): $T = 288$ K, c(1-hexene) = 0.627 mol/L, $k_{m(exp)} = 0.36$ s^{-1}, $k_{m(obs)} = 0.14$ $L\cdot(mol\cdot s)^{-1}$. (2): $T = 288$ K, c(1-hexene) = 0.748 mol/L, $k_{m(exp)} = 0.46$ s^{-1}, $k_{m(obs)} = 0.27$ $L\cdot(mol\cdot s)^{-1}$. (3): $T = 288$ K, c(1-hexene) = 0.570 mol/L, $k_{m(exp)} = 0.32$ s^{-1}, $k_{m(obs)} = 0.09$ $L\cdot(mol\cdot s)^{-1}$. Average value from run (1) to (3): $k_{m(obs)} = 0.17$ $L\cdot(mol\cdot s)^{-1}$. *1,5-Hexadiene:* (1): $T = 288$ K, c(1,5-hexadiene) = 0.980 mol/L, $k_{m(exp)} = 0.84$ s^{-1}, $k_{m(obs)} = 0.58$ $L\cdot(mol\cdot s)^{-1}$. (2): $T = 288$ K, c(1,5-hexadiene) = 0.711 mol/L, $k_{m(exp)} = 0.482$ s^{-1}, $k_{m(obs)} = 0.31$ $L\cdot(mol\cdot s)^{-1}$. Average value from run (1) and (2): $k_{m(obs)} = 0.44$ $L\cdot(mol\cdot s)^{-1}$; $k_{m(obs)}/2 = 0.22$ $L\cdot(mol\cdot s)^{-1}$ (for calculated errors see the Supporting Information).

[Dimethylsilylenebis(cyclopentadienyl)]bis(2-propenyl)zirconium, 15: To a suspension of [dimethylsilylenebis(cyclopentadienyl)]-dichlorozirconium (790 mg, 2.27 mmol) in 150 mL diethyl ether was added a solution of allylmagnesiumbromide (1.0 M in diethyl ether, 6.8 mL, 6.80 mmol) at −78 °C. The reaction mixture was, while stirring, slowly warmed to room temperature and stirred for additional 3 h at this temperature. The solvent was removed in vacuo and the residue extracted with pentane (75 mL). The insoluble magnesium salts were removed by filtration, and the yellow filtrate was concentrated until precipitation of the product set in. The precipitate was redissolved upon warming of the mixture to 40 °C for 10 min. The off-white allyl complex **15** was crystallized at −20 °C, collected by filtration, washed with cold pentane (3 mL), and dried in vacuo (450 mg, 49%, mp.: 82.1 °C). Anal. Calcd for $C_{18}H_{24}SiZr$: C, 60.11; H, 6.73. Found: C, 59.07; H, 6.51. ^{1}H NMR (200.1 MHz, C_6D_6, 300 K): $\delta = 5.66$ (quint, $^3J = 11.7$ Hz, 2H, allyl CH), 5.35, 5.23 (each m, each 4H, C_5H_4), 2.93 (d, $^3J = 11.7$ Hz, 8H, allyl CH_2), 0.26 (s, 6H, $Si(CH_3)_2$). ^{13}C NMR (50.3 MHz, C_6D_6, 300 K): $\delta = 137.4$ (allyl CH), 128.3, 116.6 (α- and β-C_5H_4), 105.7 (ipso-C_5H_4), 64.9 (allyl CH_2), −5.4 ($Si(CH_3)_2$). The dynamic (σ-allyl)−(π-allyl) automerization of complex **15** was studied by variable temperature ^{1}H NMR spectroscopy in a $CDCl_2F/CDClF_2$ solvent mixture: ^{1}H NMR (599.9 MHz, $CDCl_2F/CDF_2Cl$, 233 K): $\delta = 5.77$ (quint, $^3J = 11.7$ Hz, 2H, allyl CH), 5.57, 5.56 (each m, each 4H, C_5H_4), 2.89 (d, $^3J = 11.7$ Hz, 8H, allyl CH_2), 0.58 (s, 6H, $Si(CH_3)_2$). ^{1}H NMR (599.9 MHz, $CDCl_2F/CDF_2Cl$, 133 K): $\delta = 6.33$ (broad, 1H, σ-allyl =CH), 6.0−5.1 (broad m, 8H, C_5H_4), 5.29 (broad, 1H, π-allyl CH), 4.56, 4.41 (each broad, each 1H, σ-allyl $=CH_2$), 3.27, 3.03, 2.46 (each broad, each 1H, π-allyl CH_2), 1.89 (broad, 1H, σ-allyl CH_2), 1.71 (broad, 1H, π-allyl CH_2), 1.50 (broad, 1H, σ-allyl CH_2), 0.60, 0.49 (each broad s, each 3H, $Si(CH_3)_2$). Coalescence of the $Si(CH_3)_2$ protons is reached at ∼162 K, $\Delta\nu$ (133 K) = 63.3 Hz, $\Delta G^{\ddagger}$ (162 K) = 7.5 ± 0.5 kcal mol^{-1}.[44] 1D-TOCSY (599.9 MHz, $CDCl_2F/CDF_2Cl$, 133 K): Irradiation at $\delta = 2.46$ (π-allyl CH_2): response at $\delta = 5.29$ (π-allyl CH), 3.27, 3.03, 1.71 (each π-allyl CH_2) ppm. Irradiation at $\delta = 1.50$ (σ-allyl CH_2) ppm: response at $\delta = 6.33$ (σ-allyl =CH), 4.56, 4.41 (each σ-allyl $=CH_2$), 1.89 (σ-allyl CH_2). IR (KBr): $\tilde{\nu}$ = 3069 (w), 2958 (w), 2890 (w), 1595 (s), 1533 (w), 1400 (w), 1367 (w), 1257 (s), 1249 (s), 1053 (s), 1042 (s), 1008 (m), 902 (m), 813 (s), 807 (s), 788 (s), 754 (s), 682 (s) cm^{-1}.

[Dimethylsilylene(tetramethylcyclopentadienyl)(*tert*-butylamido)]-bis(2-propenyl)zirconium, 16. To a suspension of [dimethylsilylene-(tetramethylcyclopentadienyl)(*tert*-butylamido)]dichlorozirconium (350 mg, 0.85 mmol) in diethyl ether (30 mL) was slowly added a solution of allylmagnesiumbromide (1.11 M in ether, 1.69 mL, 1.87 mmol) at −78 °C. The reaction mixture was slowly warmed to room temperature and stirred for additional 4 h. The solvent was removed in vacuo and the residue extracted with pentane (20 mL). The insoluble magnesium salts were removed by filtration, and the clear filtrate was evaporated to dryness to yield 338 mg (94%) of the bis(allyl) complex **16** as an off-white solid. ^{1}H NMR (599.9 MHz, toluene-d_8, 298 K): $\delta = 5.82$ (quint, $^3J = 11.9$ Hz, 2H, allyl-CH), 2.96 (d, $^3J = 11.9$ Hz, 8H, allyl-CH_2), 2.09, 1.40 (each s, each 6H, $C_5(CH_3)_4$), 0.97 (s, 9H, $C(CH_3)_3$), 0.50 (s, 6H, $Si(CH_3)_2$). ^{13}C NMR (150.8 MHz, toluene-d_8, 298 K): $\delta = 143.0$ (CH, allyl-CH), 127.3, 123.7 (each C, α- and β-$\underline{C}_5(CH_3)_4$), 75.6 (CH_2, allyl-CH_2), 56.7 (C, $\underline{C}(CH_3)_3$), 33.9 (CH_3, $C(\underline{C}H_3)_3$), 15.0, 11.2 (each CH_3, $C_5(\underline{C}H_3)_4$), 7.0 ($\underline{C}H_3$, $Si(CH_3)_2$), resonance of the ipso-C of $C_5(CH_3)_4$ not detected. The dynamic (σ-allyl) ⇌ (π-allyl) automerization of complex **16** was studied by variable temperature ^{1}H NMR spectroscopy in a $CDCl_2F/CDClF_2$ solvent mixture: ^{1}H NMR (599.9 MHz, $CDCl_2F/CDClF_2$, 253 K): $\delta = 5.89$ (quint, $^3J = 11.9$ Hz, 2H, allyl-CH), 2.92 (d, $^3J = 11.9$ Hz, 8H, allyl-CH_2), 2.27, 1.74 (each s, each 6H, $C_5(CH_3)_4$), 1.08 (s, 9H, $C(CH_3)_3$), 0.60 (s, 6H, $Si(CH_3)_2$). At ∼130 K the resonance signal of the $Si(CH_3)_2$ protons splits into two signals: δ (128 K) = 0.54, 0.48 (each broad s, each 3H, $Si(CH_3)_2$) ppm. $\Delta\nu$ (128 K) = 34.3 Hz, $\Delta G^{\ddagger}$ (130 K) = 6.1 ± 0.5 kcal mol^{-1}.

Acknowledgment. Financial support from the Fonds der Chemischen Industrie, the Bundesminister für Bildung und Wissenschaft, Forschung und Technologie, and the Deutsche Forschungsgemeinschaft is gratefully acknowledged.

Supporting Information Available: Details of the NMR spectroscopic characterization of the betaine complexes and the alkene insertion products, determination of the rate constants, derivation of the kinetic expressions, and a detailed error calculation (PDF). This material is available free of charge via the Internet at http://pubs.acs.org.

JA0005338

(44) Green, M. L. H.; Wong, L.-L.; Seela, A. *Organometallics* **1992**, *11*, 2660−2668 and references therein.